Oncogene (2012) 31, 342–351

www.nature.com/onc

ORIGINAL ARTICLE

Early-stage formation of an epigenetic field defect in a mouse colitis model, and non-essential roles of T- and B-cells in DNA methylation induction

M Katsurano[1], T Niwa[1], Y Yasui[2], Y Shigematsu[1], S Yamashita[1], H Takeshima[1], MS Lee[3], Y-J Kim[3], T Tanaka[2] and T Ushijima[1]

[1]Division of Epigenomics, National Cancer Center Research Institute, Tokyo, Japan; [2]Department of Oncological Pathology, Kanazawa Medical University, Ishikawa, Japan and [3]Department of Biochemistry, Genome Regulation Center, Yonsei University, Seoul, Korea

Epigenetic fields for cancerization are involved in development of human cancers, especially those associated with inflammation and multiple occurrences. However, it is still unclear when such field defects are formed and what component of inflammation is involved in induction of aberrant DNA methylation. Here, in a mouse colitis model induced by dextran sulfate sodium (DSS), we identified three CpG islands specifically methylated in colonic epithelial cells exposed to colitis. Their methylation levels started to increase as early as 8 weeks after DSS treatment and continued to increase until colon cancers developed at 15 weeks. In contrast to the temporal profile of DNA methylation levels, infiltration of inflammatory cells spiked immediately after the DSS treatment and then gradually decreased. Exposure of cultured colonic epithelial cells to DSS did not induce DNA methylation and it was indicated that inflammation triggered by the DSS treatment was responsible for methylation induction. To clarify components of inflammation involved, severe combined immunodeficiency (SCID) mice that lack functional T- and B-cells were similarly treated. Even in SCID mice, DNA methylation, along with colon tumors, were induced at the same levels as in their background strain of mice (C.B17). Comparative analysis of inflammation-related genes showed that *Ifng*, *Il1b* and *Nos2* had expression concordant with methylation induction whereas *Il2*, *Il6*, *Il10*, *Tnf* did not. These results showed that an epigenetic field defect is formed at early stages of colitis-associated carcinogenesis and that functional T and B cells are non-essential for the formation.

Oncogene (2012) **31**, 342–351; doi:10.1038/onc.2011.241; published online 20 June 2011

Keywords: epigenetics; DNA methylation; inflammation; colon cancer; mouse

Introduction

Epigenetic alterations are critically involved in human carcinogenesis (Jones and Baylin, 2007; Esteller, 2008). Especially, DNA methylation is stably inherited upon somatic cell replication (Riggs and Xiong, 2004) and methylation of promoter CpG islands (CGIs) consistently inactivates their downstream genes, including tumor-suppressor genes, such as *CDK2A*, *HIC1* and *SOCS1* (Ushijima, 2005). In spite of its importance, inducers of aberrant DNA methylation are still not fully understood. Among the few established inducers, importance of chronic inflammation, such as ulcerative colitis, hepatitis and gastritis due to *Helicobacter pylori* infection, has been shown by multiple studies (Hsieh *et al.*, 1998; Kondo *et al.*, 2000; Issa *et al.*, 2001; Niwa *et al.*, 2010; Hur *et al.*, 2011). In addition to chronic inflammation, aging and exogenous DNA, such as viruses, have been considered as inducers (Ushijima and Okochi-Takada, 2005).

Chronic inflammation-associated cancers are characterized by frequent occurrence of multiple cancers, suggesting that non-cancerous tissues exposed to chronic inflammation have already accumulated genetic and epigenetic alterations, forming a field for cancerization (Braakhuis *et al.*, 2003; Ushijima, 2007). Accumulation of genetic alterations is difficult to assess because their frequency in non-cancerous tissues is very low (Nagao *et al.*, 2001). In contrast, aberrant DNA methylation of various genes is accumulated at high levels in non-cancerous tissues exposed to chronic inflammation (Hsieh *et al.*, 1998; Kondo *et al.*, 2000; Issa *et al.*, 2001), and such accumulation levels are correlated with cancer risk (Schulmann *et al.*, 2005; Maekita *et al.*, 2006; Nakajima *et al.*, 2006; Garrity-Park *et al.*, 2010), forming an epigenetic field for cancerization (epigenetic field defect) (Ushijima, 2007). Methylation levels of marker genes, which show high methylation levels, are correlated with those of tumor-suppressor genes, which tend to show very low methylation levels (Maekita *et al.*, 2006; Ushijima, 2007).

However, it is still unclear when such an epigenetic field defect is formed during chronic inflammation-associated carcinogenesis, and how aberrant DNA methylation is induced by chronic inflammation. As inflammation involves multiple types of cells at different

Correspondence: Dr T Ushijima, Division of Epigenomics, National Cancer Center Research Institute, Chuo-ku, Tokyo 104-0045, Japan.
E-mail: tushijim@ncc.go.jp
Received 3 September 2010; revised 12 April 2011; accepted 12 May 2011; published online 20 June 2011

time points, it is important to investigate mechanisms of how such a field defect is formed *in vivo*. Such *in vivo* analysis has been hampered by the lack of appropriate animal models in which chronic inflammation and aberrant DNA methylation are involved, except for a *Helicobacter pylori* infection-induced gastritis model in Mongolian gerbils (Niwa *et al.*, 2010; Hur *et al.*, 2011). In mouse models, aberrant DNA methylation itself has been reported in lung (Vuillemenot *et al.*, 2004), skin (Fraga *et al.*, 2004), small intestine (Hahn *et al.*, 2008), and prostate (Yamashita *et al.*, 2008) cancers and in hematological malignancies (Yu *et al.*, 2005).

In this study, we focused on a mouse colitis model induced by dextran sulfate sodium (DSS), which share some aspects with human ulcerative colitis (Rosenberg *et al.*, 2009), as a possible model in which an epigenetic field defect is involved. After identification of CGIs aberrantly methylated in azoxymethane (AOM) and DSS-induced mouse colon cancers, we clarified when aberrant DNA methylation is induced in colonic epithelial cells during colitis and what cells are critically involved in the induction.

Results

Identification of CGIs methylated in colitis-associated mouse colon tumors

We started by identifying CGIs specifically methylated in mouse colon tumors associated with colitis. AOM/DSS-induced colon tumors and untreated normal colon epithelial samples were obtained from the animal experiment described in Figure 1a. Methylated DNA immunoprecipitation (MeDIP)-CGI microarray analysis was performed using a pool of the two tumors and a pool of two normal epithelial samples, and we isolated 23 candidate CGIs methylated in the tumors. Their methylation statuses were analyzed by methylation-specific PCR (MSP) of the samples used for the MeDIP-microarray analysis, three additional colon tumors and normal epithelial samples obtained from untreated mice. Fifteen of the 23 CGIs were specifically methylated in four or more of the five tumors (Figure 1b; Table 1). The presence of densely methylated DNA molecules was further confirmed by bisulfite sequencing for three CGIs (*Fosb*, *Hoxa5* and *Krt7*) in the five tumors (Figure 1c).

DNA methylation induction in colonic epithelial cells and its temporal profiles

DNA methylation of the 15 CGIs was then analyzed in epithelial samples exposed to AOM and/or DSS by quantitative MSP (qMSP) (Figure 1d and Supplementary Figure S1). Fourteen of them had significantly increased methylation levels in epithelial samples of AOM/DSS-treated and DSS-treated mice but not in those of AOM-treated mice. This showed that DNA methylation of these CGIs was associated with DSS treatment.

Epithelial samples might be contaminated with infiltrating blood cells although they were prepared by the crypt isolation technique. We therefore analyzed methylation levels of the 14 CGIs in peripheral blood, and three (*Fosb*, *Msx1* and *Sox11*) had low methylation levels (0–5.1 percentage of the methylated reference (PMR)) whereas the other 11 CGIs had high methylation levels (11–78 PMR; shown as numbers in parentheses in Figure 1d and Supplementary Figure S1). We further purified epithelial cells and blood leukocytes by fluorescence-activated cell sorting using Epcam (a pan-epithelial cell marker) and Cd45 (a pan-leukocyte marker), respectively, from colonic epithelial samples. At 15 weeks, methylation levels of the three CGIs with low methylation in peripheral blood (*Fosb*, *Msx1*, and *Sox11*) were significantly higher in the epithelial (Epcam-positive) cells of the DSS-treated mice than in those of untreated mice (7.3- to 19.3-fold; Supplementary Figure S3). These three CGIs were located inside the genes or in the 5′ far upstream region of the gene.

Using these three CGIs, temporal profiles of methylation induction were analyzed in the course of DSS-induced colitis (Figure 2a). All the three CGIs showed gradual increases of DNA methylation levels, starting at 8 weeks after DSS treatment and reaching 7.4- to 9.2-fold high levels, compared with untreated controls, at 15 weeks (Figure 2b). When the remaining 11 CGIs with high DNA methylation levels in peripheral blood were analyzed (Supplementary Figure S2), three (*Fut4*, *Hoxa5* and *Mex3a*) showed similar profiles to the above three CGIs and eight (*5730596B20Rik*, *Bcl6b*, *Epcam*, *Fmnl1*, *Irf2bp*, *Nav1*, *Rara* and *Sh2d3c*) showed a spiked increase immediately after the DSS treatment and a gradual decrease to control levels by 15 weeks.

No induction of aberrant DNA methylation by treatment of colonic epithelial cells with DSS in vitro

DSS is known to have direct effects on epithelial cells, such as induction of cell growth arrest and production of cytokines (Ni *et al.*, 1996; Araki *et al.*, 2006), and this raised a possibility that DSS might directly induce aberrant DNA methylation in colonic epithelial cells. To address this possibility, immortalized normal mouse colonic epithelial cells (LIF-16) were treated with four concentrations of DSS that inhibited cell growth in a dose-dependent manner (Figure 3a). As the maximum dose (2%) did not affect cellular morphology (Figure 3b), the cells were cultured for 2, 5 and 8 weeks after 1 week of treatment with 2% DSS or in the presence of 2% DSS (Figure 3c). The methylation levels of the three CGIs (*Fosb*, *Msx1*, and *Sox11*) in the DSS-treated cells remained in the same range with those in untreated cells (Figure 3d). This showed that DSS itself was unlikely to induce DNA methylation in colonic epithelial cells.

Temporal profiles of inflammatory cell infiltration after the DSS treatment

In the previous study, we found that aberrant DNA methylation is induced in gastric epithelial samples exposed to specific kinds of inflammation (Hur *et al.*, 2011). Because a direct effect of DSS on methylation induction was unlikely, inflammation triggered by the

DSS treatment was suggested to be involved in the methylation induction. To identify specific inflammatory cells associated with DNA methylation induction, their infiltration was assessed by counting the number of infiltrating lymphocytes, macrophages, and neutrophils in colonic mucosae and submucosae (Figure 2c). Lymphocyte and neutrophil infiltration was most severe immediately after the DSS treatment, then gradually decreased, but was still present even at weeks 15. Macrophage infiltration stayed at high levels through-

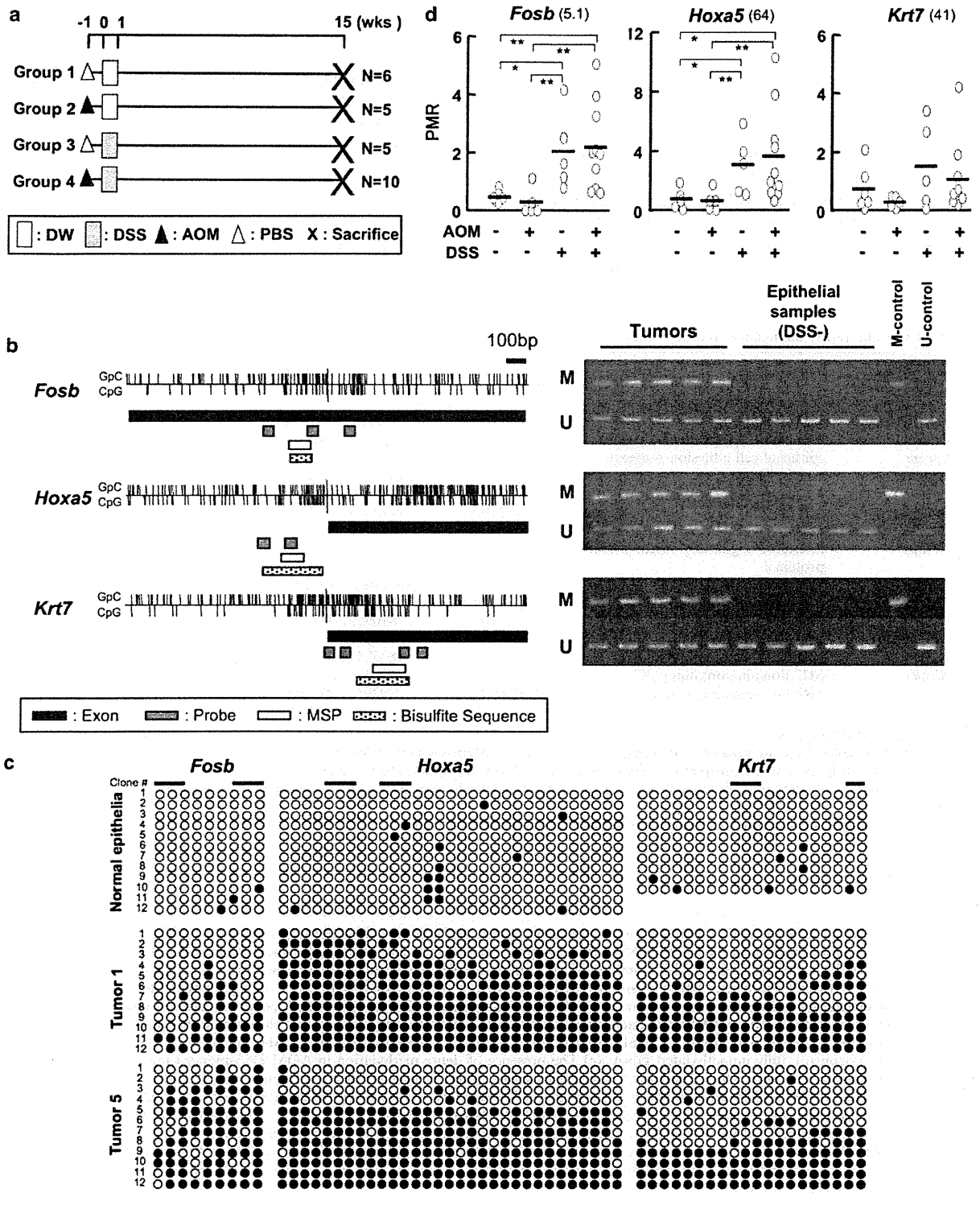

out the experimental period. These results showed that inflammation was present in the DSS-treated colon throughout the experimental period despite DSS being transiently administered, and that dominantly infiltrating cells shifted from neutrophils/lymphocytes to macrophages. The number of inflammatory cells did not parallel the temporal profiles of gradually increasing DNA methylation levels of the six CGIs (*Fosb*, *Fut4*, *Hoxa5*, *Mex3a*, *Msx1* and *Sox11*).

Carcinogenicity and DNA methylation induction in severe combined immunodeficiency mice

As the infiltration of inflammatory cells in wild-type (BALB/c) mice after DSS treatment was extensive, identification of specific inflammatory cells and inflammation-related genes responsible for DNA methylation induction was difficult. Therefore, we adopted a strategy of analyzing carcinogenicity and DNA methylation induction in severe combined immunodeficiency (SCID) mice (Figure 4a), which lack functional T- and B-cells but have normal innate immunity (Bosma *et al.*, 1983). So far, there has been no report of aberrant methylation induction by DSS colitis in SCID mice. Tumor incidence and multiplicity showed no significant difference between SCID and its wild-type control, C.B17 (Figure 4b; Table 2), demonstrating that functional T- and B-cells are not essential for tumor induction in SCID mice. Methylation of *Fosb*, *Msx1* and *Sox11* was significantly induced in colonic epithelial samples of AOM/DSS-treated SCID mice to almost the same level as those in C.B17 mice (Figure 4c), demonstrating that functional T- and B-cells are dispensable for methylation induction.

Expression of inflammation-related genes in DSS-treated SCID mice

Infiltration of inflammatory cells and expression levels of inflammation-related genes were analyzed in the

Table 1 CGIs aberrantly methylated in mouse colon tumors

	Gene symbol	*Gene name*	*Accession numbers*	*Affected CGI region*[a]	*Chromosome*	*Position*[b]
1	*5730596B20Rik*	RIKEN cDNA 5730596B20 gene	NM_175261	52106690-52106900	6	5′ Proximal upstream
2	*Bcl6b*	B-cell CLL/lymphoma 6, member B	NM_007528	70042575-70042939	11	Inside
3	*Epcam*	epithelial cell adhesion molecule	NM_008532	87548510-87548927	17	Inside
4	*Fmnl1*	formin-like 1	NM_019679	103015371-103015514	11	3′ Downstream
5	*Fosb*	FBJ osteosarcoma oncogene B	NM_008036	18463460-18463668	7	Inside
6	*Fut4*	fucosyltransferase 4	NM_010242	14501158-14501694	9	Inside
7	*Hoxa5*	homeobox A5	NM_010453	52134331-52134506	6	5′ Proximal upstream
8	*Irf2bp1*	interferon regulatory factor 2-binding protein 1	NM_178757	18163624-18163938	7	Inside
9	*Krt7*[c]	keratin 7	NM_033073	101240421-101240949	15	Inside
10	*Mex3a*	mex3 homolog A	NM_001029890	88622212-88622469	3	Inside
11	*Msx1*	homeobox, msh-like 1	NM_010835	38109507-38109773	5	Inside
12	*Nav1*	neuron navigator 1	NM_175447	137401177-137401323	1	Inside
13	*Rara*	retinoic acid receptor, alpha	NM_009024	98752420-98752549	11	5′ Far upstream
14	*Sh2d3c*	SH2 domain-containing 3C	NM_013781	32563730-32563900	2	Inside
15	*Sox11*	SRY-box-containing gene 11	NM_009234	27929531-27929660	12	5′ Far upstream

Abbreviation: CGI, CpG island.
[a]Region in the corresponding chromosome annotated by UCSC mm8 (NCBI Build 36, February 2006).
[b]Relative position to the gene (5′ far upstream, a region more than 300 bp upstream of the transcription start site; 5′ proximal upstream, a region within 300 bp upstream of the transcription start site; inside, a region in the exon or intron; and 3′ downstream, a region within 10 kbp downstream of the last exon).
[c]A gene whose methylation in non-cancerous mucosae was not significantly elevated.

Figure 1 Identification of CGIs methylated in mouse colon tumors and colonic epithelial samples exposed to DSS. (**a**) Experimental protocol of tumor induction by AOM and DSS in BALB/c mice. Tumor incidence of this experiment is summarized in Supplementary Table S1. (**b**) CpG map of a CGI, and its methylation in tumor samples (data shown for representative three CGIs). Vertical lines, individual CpG or GpC sites; open boxes, positions of MSP products; closed boxes, positions of exons; gray boxes, locations of probes in CGI microarrays; and dotted boxes, positions of bisulfite sequencing. MSP was performed using two pairs of colon tumors and normal epithelial samples without DSS treatment used for MeDIP-CGI microarray analysis and three additional pairs. M, MSP using primers specific to methylated DNA; U, MSP using primers specific to unmethylated DNA; M-control, fully methylated genomic DNA; and U-control, fully unmethylated DNA. (**c**) The presence of dense methylation in AOM/DSS-induced mouse colon tumors. Bisulfite sequencing of *Fosb*, *Hoxa5* and *Krt7* was performed in epithelial samples of an untreated mouse aged 22 weeks (group 1, weeks 15) and two AOM/DSS-induced colon tumors (group 4, weeks 15). Ten to 12 DNA molecules were analyzed per sample for a gene. Three other tumors not presented here showed similar methylation patterns. Bars, CpG sites interrogated by MSP primers; open circles, unmethylated CpG sites; and closed circles, methylated CpG sites. (**d**) DNA methylation levels in colonic epithelial samples from AOM/DSS, AOM, DSS and untreated groups. DNA methylation levels were quantified by qMSP. Bold horizontal bars indicate average. Numbers in parentheses show methylation levels in peripheral blood of mice aged 22 weeks. Methylation levels were shown to be increased by DSS treatment. $*P<0.05$; $**P<0.01$.

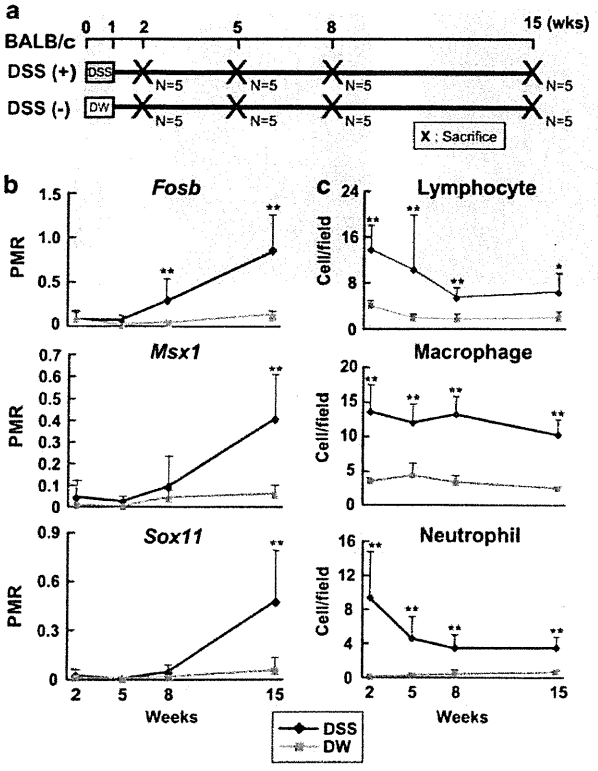

Figure 2 Temporal profiles of DNA methylation and inflammation after DSS treatment. (**a**) Experimental protocol for the time course analysis. (**b**) Temporal profiles of DNA methylation levels. (**c**) Temporal profiles of infiltration of inflammatory cells. Methylation levels and infiltration of inflammatory cells are shown as mean + s.d. $*P<0.05$; $**P<0.01$ when compared with untreated age-matched groups.

colon of DSS-treated SCID mice at 8 weeks (Figure 4a, d and e). This time point was chosen because DNA methylation was increasing at this point in the DSS-treated BALB/c mice and was considered to be actively being induced. Quantification of inflammatory cells confirmed that there was little infiltration of lymphocytes in SCID mice. In contrast, infiltration of macrophages and neutrophils were induced both in SCID and C.B17 mice by DSS treatment. Treatment with only DSS was conducted because DSS only was sufficient for methylation induction (Figure 1d and Supplementary Figure S1) and we wanted to avoid any additional expression changes caused by AOM.

Among the eight inflammation-related genes analyzed, upregulation of *Ifng*, *Il1b* and *Nos2* by DSS treatment was commonly observed in SCID and C.B17 mice (Figure 4e). On the other hand, upregulation of four genes (*Il2*, *Il6*, *Il10* and *Tnf*) was observed only in C.B17 mice, not in SCID mice. *Cox2* expression was not induced by DSS treatment either in SCID or in C.B17 mice. As inflammation-related genes upregulated commonly in SCID and C.B17 mice were likely to be involved in DNA methylation induction, *Ifng*, *Il1b* and *Nos2* were considered as candidates involved in DNA methylation induction.

Discussion

We here demonstrated that aberrant DNA methylation was induced in colonic epithelial cells as early as 8 weeks after DSS treatment, when no macroscopic tumors appeared, and the methylation level gradually increased until macroscopic tumors developed. The presence of aberrant DNA methylation in early stages of carcinogenesis was consistent with findings in *Gpx1/2* double knockout mice, a model for human inflammatory bowel disease (Hahn *et al.*, 2008) and in gastric epithelia of Mongolian gerbils exposed to *Helicobacter pylori* infection (Niwa *et al.*, 2010; Hur *et al.*, 2011). The present study is unique in that DNA methylation levels gradually increased even if inflammation gradually diminished.

To investigate components of inflammation involved in methylation induction, we utilized SCID mice, and found that DNA methylation and colon tumors were induced in them to almost the same level as those in C.B17 mice. This clearly showed that functional T- and B-cells are non-essential for DNA methylation and tumor induction. Induction of colitis by DSS in SCID mice has long been known (Dieleman *et al.*, 1994), but tumor incidence has not been analyzed. This is the first study that showed DNA methylation and tumors are induced in SCID mice by AOM and DSS to almost the same level as those in wild-type mice. In SCID mice, infiltration of macrophages and neutrophils was almost at the same levels as in C.B17 mice. Considering the importance of chronic inflammation, it was suggested that macrophages could be the proximate effector for DNA methylation induction. Among the eight inflammation-related genes examined, *Ifng*, *Il1b* and *Nos2* were upregulated by DSS treatment both in SCID and C.B17 mice.

The eight inflammation-related genes (*Cox2*, *Ifng*, *Il1b*, *Il2*, *Il6*, *Il10*, *Nos2*, and *Tnf*) examined here are known to show increased expression in inflamed human bowels (Cappello *et al.*, 1992; McLaughlan *et al.*, 1997; Autschbach *et al.*, 2002; Li *et al.*, 2009; Wang and Dubois, 2010). Especially, IL1β is produced at significantly high levels also in human ulcerative colitis (Ligumsky *et al.*, 1990). *In vitro*, administration of IL1β is reported to induce DNA methylation through induction of *Nos2* (Hmadcha *et al.*, 1999) and in *CDH1* promoter (Qian *et al.*, 2008). INFγ is reported to be involved in initiation of DSS-induced colitis (Ito *et al.*, 2006) and in development of colon tumors in *Socs1*-deficient mice (Hanada *et al.*, 2006), but its role in induction of aberrant DNA methylation is still unknown. Il6 is known to induce DNA methyltransferase expression (Hodge *et al.*, 2001), and its deficiency in mice leads to decreased tumor number and size after AOM and DSS treatment (Grivennikov *et al.*, 2009). *Il2* and *Il10* deficiency in mice leads to development of spontaneous colitis (Kuhn *et al.*, 1993; Sadlack *et al.*, 1993). Blocking of *Tnf* signal reduced tumor number after AOM and DSS treatment (Popivanova *et al.*, 2008).

Technically, the MeDIP-CGI microarray analysis isolated 23 candidate CGIs methylated in primary

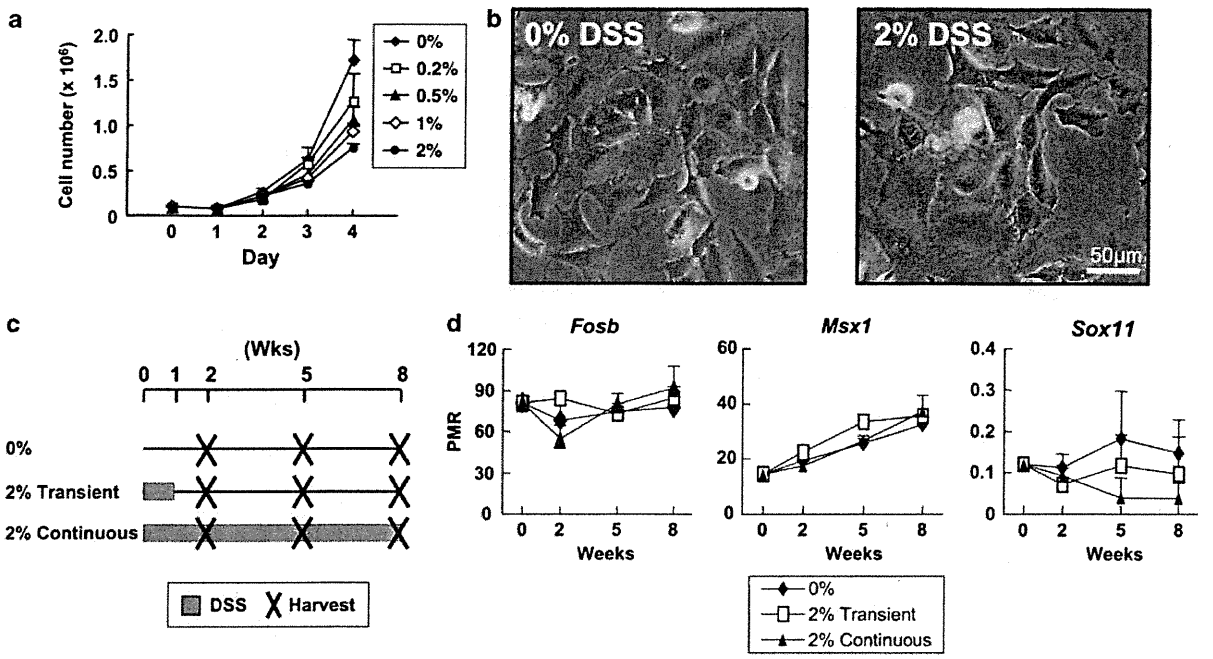

Figure 3 Direct effects of DSS on methylation induction. (**a**) Effect of four doses of DSS on cellular growth. Numbers are shown as mean + s.d. of three independent cultures. (**b**) Morphology of the cells (day 2). No morphological changes were induced with the highest dose. (**c**) Experimental protocol for time course methylation analysis. (**d**) Methylation levels in the DSS-treated epithelial cells. Cells on day 0 denote original cells before the plating. Methylation levels are shown as mean + s.d. of three independent cultures. DSS did not induce methylation directly, even after 8-week culture, although it affected the cellular growth.

mouse colon tumors. The number was smaller than expected from the known finding that 170–621 CGIs are methylated in human colon cancers (Keshet *et al.*, 2006; Kim *et al.*, 2011). However, using the same cutoff values used in this study, we were able to isolate 2339 methylated CGIs in a mouse colon cancer cell line, Colon26 (data not shown). Therefore, it was unlikely that there was a technical problem, and it was suggested that the mouse primary colon tumors had much smaller numbers of methylated CGIs than the Colon26 mouse colon cancer cell line and human colon cancers.

In summary, by DSS-induced inflammation, aberrant DNA methylation was shown to start to accumulate in epithelial cells at early stages of carcinogenesis. T- and B-cells were non-essential for DNA methylation induction.

Materials and methods

Cell line and DSS treatment

LIF-16, an embryonic colonic epithelial cell line established from *Trp53*$^{-/-}$ mice as described previously (Taniwaki *et al.*, 2007), was kindly provided by Dr Hiroshi Fukamachi at Tokyo Medical and Dental University and maintained in Dulbecco's modified Eagle's medium supplemented with 10% fetal bovine serum. For cell growth assay, 10^5 cells were plated. After attachment of the cells, the culture media were replaced by those containing DSS (molecular weight = 36 000–50 000; MP Biochemicals, Solon, OH, USA). The cell number was counted by a Countess automated cell counter (Invitrogen, Rockville, MD, USA). For methylation assay, 5×10^3 cells were plated on 6 cm dishes. Every third or fourth day, the cells were passaged using Dulbecco's modified Eagle's medium without DSS, and DSS was added after attachment of the cells during the duration described in Figure 3c.

Animals and cancer induction experiments

Male BALB/c mice were purchased from Charles River Laboratories (Yokohama, Japan). Male C.B17/Icr-scid/scid (SCID) and C.B17/Icr-$^{+/+}$ (C.B17) mice were purchased from CLEA Japan (Tokyo, Japan). AOM (10 mg/kg body weight; NARD Institute, Amagasaki, Japan) or phosphate-buffered saline (PBS) was administered by single intraperitoneal injection. DSS (molecular weight = 36 000–50 000) was administered to mice at 6 or 7 weeks of age in drinking water at a concentration of 1.5 or 2.0% w/v. Colon cancers and colonic epithelial samples for MeDIP-CGI microarray analysis were obtained from BALB/c mice treated with AOM and DSS (Figure 1a; Supplementary Table S1), which showed similar carcinogenicity to our previous reports (Tanaka *et al.*, 2003). All the animal experiments were approved by the Committee for Ethics in Animal Experimentation at the National Cancer Center.

Sample preparation

The large bowel was cut open longitudinally and the number of macroscopic tumors whose major axes were more than 3 mm was counted. Large tumors were collected and half of each tumor was fixed with neutralized 10% formalin for histological analysis and the other half was kept frozen for

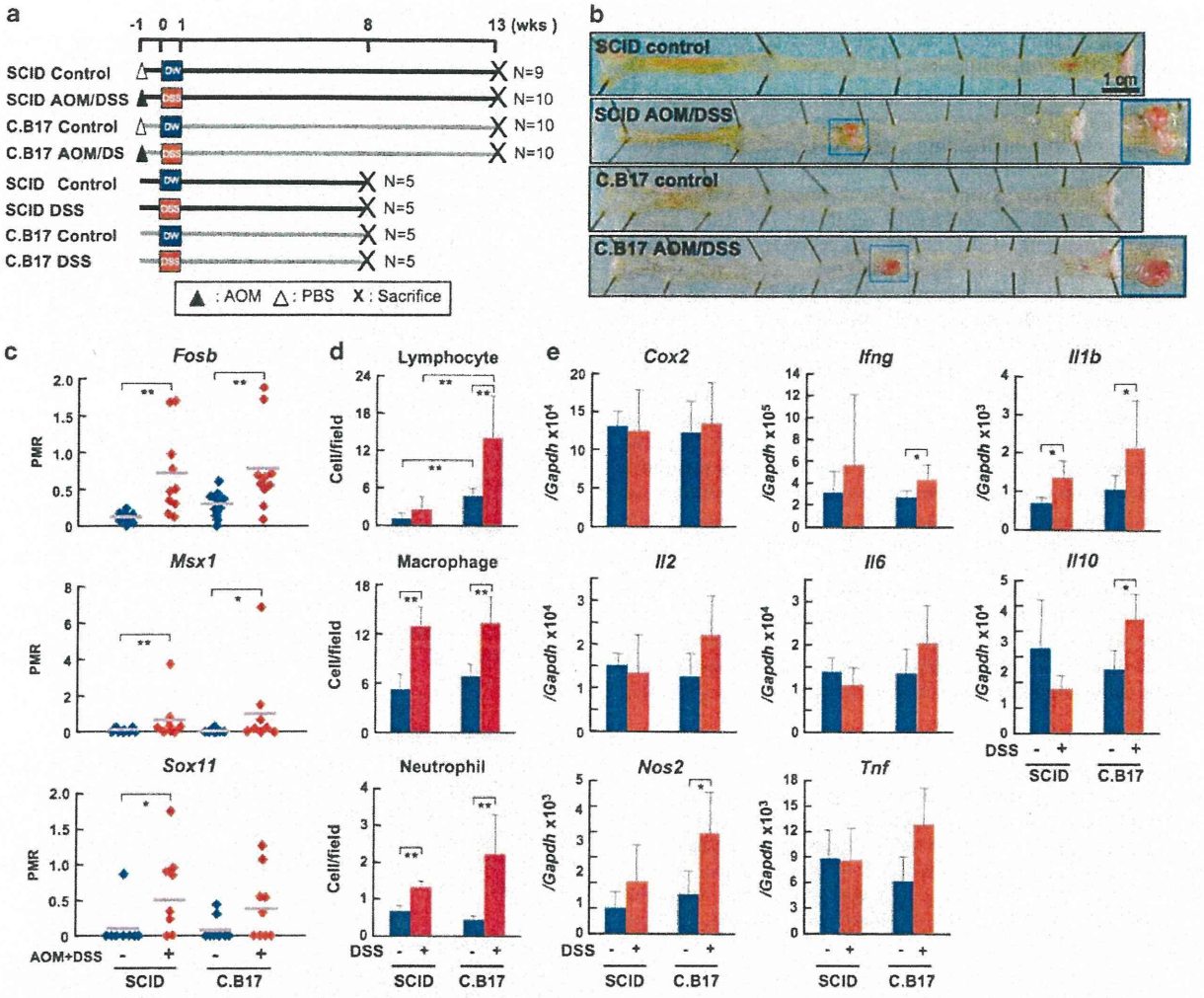

Figure 4 Tumor and DNA methylation induction in SCID mice. (**a**) Experimental protocol for AOM/DSS treatment in SCID and C.B17 mice. (**b**) Representative macroscopic appearance of the colon in the four groups. Colon tumors were induced at the same incidence in C.B17 and SCID mice. Right panels are the magnified view of tumors in blue rectangles. (**c**) DNA methylation levels at 13 weeks after DSS treatment. The levels were analyzed by qMSP of colonic epithelial samples from SCID and C.B17 mice treated with or without AOM/DSS. Bold horizontal bars indicate average. Similar levels of DNA methylation were induced in both SCID and C.B17 mice. (**d**) Infiltration of inflammatory cells and (**e**) expression levels of inflammation-related genes 8 weeks after DSS treatment in colonic tissues of SCID and C.B17 mice. Infiltration of inflammatory cells and gene expression levels are shown as mean + s.d. $^{*}P<0.05$; $^{**}P<0.01$.

Table 2 Tumor incidence and multiplicity in SCID and C.B17 mice

Strain	*Treatment*	*Incidence (%)*	*Number of tumors/mouse bearing tumors*[a]	*Size*[b]
SCID	AOM/DSS	9/10 (90)	2.8 ± 1.6	4.2 ± 0.69
	Control	0/9 (0)	—	—
C.B17	AOM/DSS	10/10 (100)	2.1 ± 1.2	4.6 ± 0.89
	Control	0/10 (0)	—	—

Abbreviations: AOM, azoxymethane; DSS, dextran sulfate sodium; SCID, severe combined immunodeficiency.
[a]Mean ± s.d.
[b]Mean ± s.d. in the major axis.

DNA and RNA isolation. Colonic epithelial samples were isolated from distal large bowels by the crypt isolation technique (Cheng *et al.*, 1984). Briefly, the distal half of the large bowel was incubated in a Hanks' balanced salt solution with 30 mM EDTA at 37 °C for 10 min. After the incubation, epithelium was collected by scraping off gently and washed with PBS. Peripheral blood was obtained from the inferior vena cava of DSS-treated and non-treated mice at 22 weeks of age.

Fluorescence-activated cell sorting
To dissociate single cells, epithelial samples were incubated in Hanks' balanced salt solution containing 10 mM HEPES (pH7.3), 1 mg/ml collagenase D (Roche Diagnostics, Penzberg, Germany) and 25 μg/mL DNase I (Sigma-Aldrich, St Louis, MO, USA) at 37 °C for 80 min with gentle agitation. The cells were washed with PBS and then fixed with 80% acetone at 4 °C for 5 min. After washing with PBS, the fixed cells were incubated with a phycoerythrin-labeled anti-mouse Epcam antibody (eBiosciense, San Diego, CA, USA) and a

fluorescein isothiocyanate-labeled anti-Cd45 antibody (Miltenyi Biotech, Auburn, CA, USA) and sorted by FACSAria II cell sorter (BD, Franklin Lakes, NJ, USA).

Histological analysis
Macrophages and neutrophils were detected by immunohistochemistry of formalin-fixed tissues using a rabbit anti-F4/80 antibody (Santa Cruz Biotechnology, Santa Cruz, CA, USA) and a rat anti-Ly6G antibody (Thermo Fisher Scientific, Fremont, CA, USA), respectively, as primary antibodies. Sections of 3 μm thickness were rehydrated and incubated in 10 mM citrate buffer (pH 6) at 120 °C for 5 min to unmask the antigen. After blocking with 0.5% bovine serum albumin in PBS, sections were incubated with each primary antibody overnight. The immune complex was visualized by a Vectastain Elite ABC kit (Vector Laboratories, Burlingame, CA, USA) and the sections were stained with hematoxylin. Mononuclear cells without F4/80 staining were considered as lymphocytes. The numbers of neutrophils, macrophages and lymphocytes in mucosae and submucosae were counted under 400 × magnification across seven random fields per colon. For immunofluorescent microscopy, fresh colonic tissues were embedded in O.T.C. compound (Sakura Finetek, Tokyo, Japan) and frozen by liquid nitrogen. Sections of 3 μm thickness were prepared and fixed with acetone at −20 °C for 5 min. The hydrated sections were incubated with the phycoerythrin-labeled anti-mouse Epcam antibody and the fluorescein isothiocyanate-labeled anti-Cd45 antibody.

Nucleic acid isolation
From colonic epithelial samples and cells purified by fluorescence-activated cell sorting, genomic DNA was extracted by the standard phenol/chloroform method, and RNA was isolated using ISOGEN (Nippon Gene, Tokyo, Japan). Genomic DNA of peripheral blood was extracted by a QuickGene DNA whole blood kit (Fujifilm, Tokyo, Japan).

MeDIP-CGI microarray
MeDIP-CGI microarray analysis was performed as previously described (Takeshima *et al.*, 2009; Yamashita *et al.*, 2009). Briefly, to immunoprecipitate methylated DNA, 5 μg of sonicated genomic DNA was incubated with an anti-5-methylcytidine antibody (Diagenode, Lié, Belgium) at 4 °C overnight. Immune complexes were collected with Dynabeads Protein A (Invitorogen Dynal AS, Oslo, Norway) and digested with proteinase K. Immunoprecipitated DNA was purified by phenol/chloroform extraction and isopropanol precipitation. Using an Agilent Genomic DNA Labeling Kit PLUS (Agilent Technologies, Santa Clara, CA, USA), the precipitated and input DNAs were labeled with Cy5 and Cy3, respectively, without any amplification. Labeled DNA was hybridized to a mouse CGI oligonucleotide microarray (Agilent Technologies) containing 97 652 probes covering 16 030 CGIs at 67 °C for 40 h with constant rotation and then scanned with an Agilent G2565BA microarray scanner (Agilent Technologies). Scanned data were processed with Feature Extraction Ver.9.1 and Agilent G4477AA ChIP Analytics 1.3 software (Agilent Technologies). Probes with signal log ratio $\geqslant 0.5$ in a tumor sample and $\leqslant -0.2$ in a normal sample were considered to be methylated, and CGIs in which two or more continuous probes were methylated and at least one probe had a normalized log ratio more than 1.2 were considered as methylated.

MSP, qMSP and bisulfite sequencing
Bisulfite modification was performed using 1 μg of *Bam*HI-digested genomic DNA as previously described (Yamashita *et al.*, 2008). The sample was resuspended in 40 μl of Tris–EDTA buffer, and an aliquot of 1 μl was used for MSP (qMSP) and bisulfite sequencing. Fully methylated and fully unmethylated DNA were prepared by amplifying mouse genomic DNA with GenomiPhi and by methylating it with *Sss*I methylase, respectively (Niwa *et al.*, 2005). Primers for MSP (Supplementary Table S2) were designed within ~100 bp from methylated probes. Primers for bisulfite sequencing were designed to cover the region amplified by MSP (Supplementary Table S2). qMSP was performed by real-time PCR using SYBR Green I (BioWhittaker Molecular Applications, Rockland, ME, USA) and an iCycler Thermal Cycler (Bio-Rad Laboratories, Hercules, CA, USA) in duplicate. The number of molecules in a sample was determined by comparing its amplification with those of standard DNA prepared by purification of PCR products. The number was highly reproducible using the same samples (correlation coefficient >0.8). DNA methylation levels were expressed as a PMR, which reflected a fraction of the DNA molecules methylated at a specific locus (Kass *et al.*, 1997; Niwa *et al.*, 2010). PMR was calculated as ((no of molecules methylated at a target CGI in a sample)/(no of B2 SINE repeat in the sample))/((no of molecules methylated at the target CGI in a *SssI*-treated DNA)/(no of B2 SINE repeat in the *SssI*-treated DNA)) × 100.

Reverse transcriptase–PCR
Complementary DNA was synthesized from 2 μg of total RNA using a Superscript III kit (Invitrogen) with oligo dT primer. Real-time PCR was performed with gene-specific primers (Supplementary Table 3) as described in qMSP. The complementary DNA quantity of each gene was normalized to that of *Gapdh*.

Statistical analysis
Differences in DNA methylation and expression levels were analyzed by the Mann–Whitney *U* test using SPSS 13.0J. (SPSS Japan Inc., Tokyo, Japan).

Conflict of interest

The authors declare no conflict of interest.

Acknowledgements

We thank Dr H Fukamachi for his kind provision of the LIF-16 cell line. This study was supported by the Third-term Comprehensive Cancer Control Strategy from the Ministry of Health, Labour and Welfare, Japan; and by the Global Research Laboratory Program from Korea Foundation for International Cooperation of Science & Technology. MK and YS are recipients of Research Resident Fellowships from the Foundation for Promotion of Cancer Research. This study was supported by the Third-term Comprehensive Cancer Control Strategy from the Ministry of Health, Labour and Welfare, Japan (TU), and by the Global Research Laboratory Program from Korea Foundation for International Cooperation of Science & Technology (Y-JK and TU).

References

Araki Y, Sugihara H, Hattori T. (2006). *In vitro* effects of dextran sulfate sodium on a Caco-2 cell line and plausible mechanisms for dextran sulfate sodium-induced colitis. *Oncol Rep* **16**: 1357–1362.

Autschbach F, Giese T, Gassler N, Sido B, Heuschen G, Heuschen U *et al.* (2002). Cytokine/chemokine messenger-RNA expression profiles in ulcerative colitis and Crohn's disease. *Virchows Arch* **441**: 500–513.

Bosma GC, Custer RP, Bosma MJ. (1983). A severe combined immunodeficiency mutation in the mouse. *Nature* **301**: 527–530.

Braakhuis BJ, Tabor MP, Kummer JA, Leemans CR, Brakenhoff RH. (2003). A genetic explanation of Slaughter's concept of field cancerization: evidence and clinical implications. *Cancer Res* **63**: 1727–1730.

Cappello M, Keshav S, Prince C, Jewell DP, Gordon S. (1992). Detection of mRNAs for macrophage products in inflammatory bowel disease by *in situ* hybridisation. *Gut* **33**: 1214–1219.

Cheng H, Bjerknes M, Amar J. (1984). Methods for the determination of epithelial cell kinetic parameters of human colonic epithelium isolated from surgical and biopsy specimens. *Gastroenterology* **86**: 78–85.

Dieleman LA, Ridwan BU, Tennyson GS, Beagley KW, Bucy RP, Elson CO. (1994). Dextran sulfate sodium-induced colitis occurs in severe combined immunodeficient mice. *Gastroenterology* **107**: 1643–1652.

Esteller M. (2008). Epigenetics in cancer. *N Engl J Med* **358**: 1148–1159.

Fraga MF, Herranz M, Espada J, Ballestar E, Paz MF, Ropero S *et al.* (2004). A mouse skin multistage carcinogenesis model reflects the aberrant DNA methylation patterns of human tumors. *Cancer Res* **64**: 5527–5534.

Garrity-Park MM, Loftus Jr EV., Sandborn WJ, Bryant SC, Smyrk TC. (2010). Methylation Status of Genes in Non-Neoplastic Mucosa From Patients With Ulcerative Colitis-Associated Colorectal Cancer. *Am J Gastroenterol.*

Grivennikov S, Karin E, Terzic J, Mucida D, Yu GY, Vallabhapurapu S *et al.* (2009). IL-6 and Stat3 are required for survival of intestinal epithelial cells and development of colitis-associated cancer. *Cancer Cell* **15**: 103–113.

Hahn MA, Hahn T, Lee DH, Esworthy RS, Kim BW, Riggs AD *et al.* (2008). Methylation of polycomb target genes in intestinal cancer is mediated by inflammation. *Cancer Res* **68**: 10280–10289.

Hanada T, Kobayashi T, Chinen T, Saeki K, Takaki H, Koga K *et al.* (2006). IFNgamma-dependent, spontaneous development of colorectal carcinomas in SOCS1-deficient mice. *J Exp Med* **203**: 1391–1397.

Hmadcha A, Bedoya FJ, Sobrino F, Pintado E. (1999). Methylation-dependent gene silencing induced by interleukin 1beta via nitric oxide production. *J Exp Med* **190**: 1595–1604.

Hodge DR, Xiao W, Clausen PA, Heidecker G, Szyf M, Farrar WL. (2001). Interleukin-6 regulation of the human DNA methyltransferase (HDNMT) gene in human erythroleukemia cells. *J Biol Chem* **276**: 39508–39511.

Hsieh CJ, Klump B, Holzmann K, Borchard F, Gregor M, Porschen R. (1998). Hypermethylation of the p16INK4a promoter in colectomy specimens of patients with long-standing and extensive ulcerative colitis. *Cancer Res* **58**: 3942–3945.

Hur K, Niwa T, Toyoda T, Tsukamoto T, Tatematsu M, Yang HK *et al.* (2011). Insufficient role of cell proliferation in aberrant DNA methylation induction and involvement of specific types of inflammation. *Carcinogenesis* **32**: 35–41.

Issa JP, Ahuja N, Toyota M, Bronner MP, Brentnall TA. (2001). Accelerated age-related CpG island methylation in ulcerative colitis. *Cancer Res* **61**: 3573–3577.

Ito R, Shin-Ya M, Kishida T, Urano A, Takada R, Sakagami J *et al.* (2006). Interferon-gamma is causatively involved in experimental inflammatory bowel disease in mice. *Clin Exp Immunol* **146**: 330–338.

Jones PA, Baylin SB. (2007). The epigenomics of cancer. *Cell* **128**: 683–692.

Kass DH, Kim J, Rao A, Deininger PL. (1997). Evolution of B2 repeats: the muroid explosion. *Genetica* **99**: 1–13.

Keshet I, Schlesinger Y, Farkash S, Rand E, Hecht M, Segal E *et al.* (2006). Evidence for an instructive mechanism of *de novo* methylation in cancer cells. *Nat Genet* **38**: 149–153.

Kim YH, Lee HC, Kim SY, Yeom YI, Ryu KJ, Min BH *et al.* (2011). Epigenomic analysis of aberrantly methylated genes in colorectal cancer identifies genes commonly affected by epigenetic alterations. *Ann Surg Oncol* (doi:10.1245/s10434-011-1573-y).

Kondo Y, Kanai Y, Sakamoto M, Mizokami M, Ueda R, Hirohashi S. (2000). Genetic instability and aberrant DNA methylation in chronic hepatitis and cirrhosis—A comprehensive study of loss of heterozygosity and microsatellite instability at 39 loci and DNA hypermethylation on 8 CpG islands in microdissected specimens from patients with hepatocellular carcinoma. *Hepatology* **32**: 970–979.

Kuhn R, Lohler J, Rennick D, Rajewsky K, Muller W. (1993). Interleukin-10-deficient mice develop chronic enterocolitis. *Cell* **75**: 263–274.

Li Y, de Haar C, Chen M, Deuring J, Gerrits MM, Smits R *et al.* (2009). Disease-related expression of the IL-6/STAT3/SOCS3 signaling pathway in ulcerative colitis and ulcerative colitis-related carcinogenesis. *Gut* **59**: 227–235.

Ligumsky M, Simon PL, Karmeli F, Rachmilewitz D. (1990). Role of interleukin 1 in inflammatory bowel disease—enhanced production during active disease. *Gut* **31**: 686–689.

Maekita T, Nakazawa K, Mihara M, Nakajima T, Yanaoka K, Iguchi M *et al.* (2006). High levels of aberrant DNA methylation in Helicobacter pylori-infected gastric mucosae and its possible association with gastric cancer risk. *Clin Cancer Res* **12**: 989–995.

McLaughlan JM, Seth R, Vautier G, Robins RA, Scott BB, Hawkey CJ *et al.* (1997). Interleukin-8 and inducible nitric oxide synthase mRNA levels in inflammatory bowel disease at first presentation. *J Pathol* **181**: 87–92.

Nagao M, Ochiai M, Okochi E, Ushijima T, Sugimura T. (2001). LacI transgenic animal study: relationships among DNA-adduct levels, mutant frequencies and cancer incidences. *Mutat Res* **477**: 119–124.

Nakajima T, Maekita T, Oda I, Gotoda T, Yamamoto S, Umemura S *et al.* (2006). Higher methylation levels in gastric mucosae significantly correlate with higher risk of gastric cancers. *Cancer Epidemiol Biomarkers Prev* **15**: 2317–2321.

Ni J, Chen SF, Hollander D. (1996). Effects of dextran sulphate sodium on intestinal epithelial cells and intestinal lymphocytes. *Gut* **39**: 234–241.

Niwa T, Tsukamoto T, Toyoda T, Mori A, Tanaka H, Maekita T *et al.* (2010). Inflammatory processes triggered by *Helicobacter pylori* infection cause aberrant DNA methylation in gastric epithelial cells. *Cancer Res* **70**: 1430–1440.

Niwa T, Yamashita S, Tsukamoto T, Kuramoto T, Nomoto T, Wakazono K *et al.* (2005). Whole-genome analyses of loss of heterozygosity and methylation analysis of four tumor-suppressor genes in N-methyl-N'-nitro-N-nitrosoguanidine-induced rat stomach carcinomas. *Cancer Sci* **96**: 409–413.

Popivanova BK, Kitamura K, Wu Y, Kondo T, Kagaya T, Kaneko S *et al.* (2008). Blocking TNF-alpha in mice reduces colorectal carcinogenesis associated with chronic colitis. *J Clin Invest* **118**: 560–570.

Qian X, Huang C, Cho CH, Hui WM, Rashid A, Chan AO. (2008). E-cadherin promoter hypermethylation induced by interleukin-1beta treatment or H. pylori infection in human gastric cancer cell lines. *Cancer Lett* **263**: 107–113.

Riggs AD, Xiong Z. (2004). Methylation and epigenetic fidelity. *Proc Natl Acad Sci USA* **101**: 4–5.

Rosenberg DW, Giardina C, Tanaka T. (2009). Mouse models for the study of colon carcinogenesis. *Carcinogenesis* **30**: 183–196.

Sadlack B, Merz H, Schorle H, Schimpl A, Feller AC, Horak I. (1993). Ulcerative colitis-like disease in mice with a disrupted interleukin-2 gene. *Cell* **75**: 253–261.

Schulmann K, Sterian A, Berki A, Yin J, Sato F, Xu Y *et al.* (2005). Inactivation of p16, RUNX3, and HPP1 occurs early in Barrett's-associated neoplastic progression and predicts progression risk. *Oncogene* **24**: 4138–4148.

Takeshima H, Yamashita S, Shimazu T, Niwa T, Ushijima T. (2009). The presence of RNA polymerase II, active or stalled, predicts epigenetic fate of promoter CpG islands. *Genome Res* **19**: 1974–1982.

Tanaka T, Kohno H, Suzuki R, Yamada Y, Sugie S, Mori H. (2003). A novel inflammation-related mouse colon carcinogenesis model induced by azoxymethane and dextran sodium sulfate. *Cancer Sci* **94**: 965–973.

Taniwaki K, Fukamachi H, Komori K, Ohtake Y, Nonaka T, Sakamoto T *et al.* (2007). Stroma-derived matrix metalloproteinase (MMP)-2 promotes membrane type 1-MMP-dependent tumor growth in mice. *Cancer Res* **67**: 4311–4319.

Ushijima T. (2005). Detection and interpretation of altered methylation patterns in cancer cells. *Nat Rev Cancer* **5**: 223–231.

Ushijima T. (2007). Epigenetic field for cancerization. *J Biochem Mol Biol* **40**: 142–150.

Ushijima T, Okochi-Takada E. (2005). Aberrant methylations in cancer cells: where do they come from? *Cancer Sci* **96**: 206–211.

Vuillemenot BR, Pulling LC, Palmisano WA, Hutt JA, Belinsky SA. (2004). Carcinogen exposure differentially modulates RAR-beta promoter hypermethylation, an early and frequent event in mouse lung carcinogenesis. *Carcinogenesis* **25**: 623–629.

Wang D, Dubois RN. (2010). The role of COX-2 in intestinal inflammation and colorectal cancer. *Oncogene* **29**: 781–788.

Yamashita S, Hosoya K, Gyobu K, Takeshima H, Ushijima T. (2009). Development of a novel output value for quantitative assessment in methylated DNA immunoprecipitation-CpG island microarray analysis. *DNA Res* **16**: 275–286.

Yamashita S, Takahashi S, McDonell N, Watanabe N, Niwa T, Hosoya K *et al.* (2008). Methylation silencing of transforming growth factor-beta receptor type II in rat prostate cancers. *Cancer Res* **68**: 2112–2121.

Yu L, Liu C, Vandeusen J, Becknell B, Dai Z, Wu YZ *et al.* (2005). Global assessment of promoter methylation in a mouse model of cancer identifies ID4 as a putative tumor-suppressor gene in human leukemia. *Nat Genet* **37**: 265–274.

Supplementary Information accompanies the paper on the Oncogene website (http://www.nature.com/onc)

Genomics 98 (2011) 182–188

Contents lists available at ScienceDirect

Genomics

journal homepage: www.elsevier.com/locate/ygeno

Effects of genome architecture and epigenetic factors on susceptibility of promoter CpG islands to aberrant DNA methylation induction

Hideyuki Takeshima [a], Satoshi Yamashita [a], Taichi Shimazu [b], Toshikazu Ushijima [a,*]

[a] Division of Epigenomics, National Cancer Center Research Institute, 5-1-1 Tsukiji, Chuo-ku, 104-0045, Tokyo, Japan
[b] Epidemiology and Prevention Division, Research Center for Cancer Prevention and Screening, National Cancer Center, 5-1-1 Tsukiji, Chuo-ku, 104-0045, Tokyo, Japan

ARTICLE INFO

Article history:
Received 28 January 2011
Accepted 2 June 2011
Available online 12 June 2011

Keywords:
Cancer
Epigenetics
DNA methylation
Target gene specificity
SINE
LINE

ABSTRACT

Aberrant DNA methylation is induced at specific promoter CpG islands (CGIs) in contrast with mutations. The specificity is influenced by genome architecture and epigenetic factors, but their relationship is still unknown. In this study, we isolated promoter CGIs susceptible and resistant to aberrant methylation induction during prostate and breast carcinogenesis. The effect of genome architecture was more evident for promoter CGIs susceptible in both of the two tissues than for promoter CGIs susceptible only in one tissue. Multivariate analysis of promoter CGIs with tissue-nonspecific susceptibility showed that genome architecture, namely a remote location from SINE (OR = 5.98; 95% CI = 2.33–15.34) and from LINE (OR = 2.08; 95% CI = 1.03–4.21), was associated with increased susceptibility, independent of epigenetic factors such as the presence of RNA polymerase II (OR = 0.09; 95% CI = 0.02–0.48) and H3K27me3 (OR = 3.28; 95% CI = 1.17–9.21). These results showed that methylation susceptibility of promoter CGIs is determined both by genome architecture and epigenetic factors, independently.

1. Introduction

Epigenetic modifications play critical roles in diverse biological processes such as transcription and DNA repair [1–3], and their alterations are involved in human disorders, including cancers [4,5]. In particular, aberrant DNA methylation of promoter CpG islands (CGIs), especially of nucleosome-free regions (NFRs), causes silencing of multiple genes, including tumor suppressor genes [6–8], and is deeply involved in human carcinogenesis [4,5]. Contrary to mutations, aberrant methylation is known to be induced at specific genes by specific inducers [9,10]. The presence of such specificity was convincingly shown by methylation analyses of polyclonal tissues, such as gastric mucosae of people with *Helicobacter pylori* infection [9] and esophageal mucosae of patients with smoking history [10]. Subsequently, by methylated DNA immunoprecipitation (MeDIP) and human CGI microarray analyses of multiple cancer cell lines and their normal counterpart cells, we showed that some promoter CGIs are susceptible across tissues (tissue-nonspecifically) to methylation induction while others are tissue-specifically susceptible [11].

As for the mechanisms of the target gene specificity, transcription levels and epigenetic factors have been known to be involved. Initially, involvement of low transcription levels was implicated by analysis of specific genes [12–15] and then demonstrated by a genome-wide analysis [11]. The premarking of DNA methylation-susceptible genes by trimethylation of histone H3 lysine27 (H3K27me3), a DNA methylation-independent repressive modification [16], was initially implicated by analysis of a limited number of genes [17,18], and then demonstrated by genome-wide analyses [11,19,20]. We recently demonstrated that the presence of RNA polymerase II (Pol II) protects promoter CGIs from becoming methylated, even if their downstream genes are not actively transcribed (stalled Pol II) [11,21]. Some transcription factors, such as NRF1, Sp1, and YY1, have also been shown to protect promoter CGIs from becoming methylated [22].

In contrast to epigenetic factors, only a limited number of reports are available for the involvement of genome architecture in DNA methylation susceptibility of promoter CGIs. A pioneering work by Feltus et al. identified genomic motives associated with methylation-susceptible and -resistant CGIs, and showed that motives associated with methylation-resistant genes tended to be associated with Alu, the major human short interspersed elements (SINE), and other repetitive sequences [23]. A recent work by Estécio et al. showed that, compared with methylation-resistant genes, methylation-susceptible genes have a lower frequency of SINE and long interspersed element (LINE) retrotransposons near their transcription start sites (TSSs) [24]. However, it is still unknown whether the effects of genome architecture are independent from those of epigenetic factors,

Abbreviations: CGI, CpG island; Pol II, RNA polymerase II; NFR, nucleosome free region; MeDIP, methylated DNA immunoprecipitation; H3K27me3, trimethylation of histone H3 lysine27; H3Ac, acetylation of histone H3; H3K4me3, trimethylation of histone H3 lysine4; H3K9me3, trimethylation of histone H3 lysine9; SINE, short interspersed element; LINE, long interspersed element.

* Corresponding author. Fax: +81 3 5565 1753.
E-mail address: tushijim@ncc.go.jp (T. Ushijima).

0888-7543/$ – see front matter © 2011 Elsevier Inc. All rights reserved.
doi:10.1016/j.ygeno.2011.06.003

especially the presence of Pol II, and how strongly it influences tissue-nonspecifically and tissue-specifically susceptible promoter CGIs.

In this study, we will first confirm that DNA methylation-susceptible promoter CGIs were located more remotely from SINE and LINE than resistant promoter CGIs. We will then show i) that the effect of genome architecture was more evident for tissue-nonspecific susceptibility than for tissue-specific susceptibility, and ii) that the effect of genome architecture was independent from those of epigenetic factors such as the presence of Pol II and H3K27me3.

2. Results

2.1. Promoter CGIs are classified into those susceptible and resistant to aberrant DNA methylation induction

Susceptibility of promoter CGIs of genes to aberrant DNA methylation induction was determined based on methylation statuses in two normal cells and five cancer cell lines in the prostate and mammary glands. Promoter CGIs unmethylated (Me value, 0–0.4) in both of the two normal cells and methylated (Me value, 0.6–1.0) in one to five of the five cancer cell lines were classified into Groups S1 to S5, respectively. Those unmethylated in both of the two normal cells and also in all of the five cancer cell lines were classified into Group R (Fig. 1A). Those unmethylated in both of the two normal cells and intermediately methylated (Me value, 0.4–0.6) at least in one of the five cancer cell lines were classified into the intermediate group (Group Int). Promoter CGIs in Groups S2 to S5 were considered to be susceptible, and those in Group R were considered to be resistant. A total of 262 and 280 promoter CGIs were classified as susceptible in the prostate and mammary glands, respectively, and 5194 and 5352 promoter CGIs, respectively, were as resistant. House-keeping genes with abundant expression and promoter CGIs, such as *GAPDH* and *ACTB*, belonged to the resistant genes.

2.2. Promoter CGIs susceptible to aberrant DNA methylation induction are located remotely from SINE and LINE

The effect of genome architecture on DNA methylation susceptibility was analyzed using the distance between a promoter CGI and SINE (or LINE) (Fig. 2A). In the prostate, susceptible promoter CGIs (n = 262) were located more remotely from SINE ($P<1\times10^{-5}$) and LINE ($P<1\times10^{-5}$) than resistant ones (n = 5194) (Figs. 2B and D). The same difference was observed in the mammary glands ($P<1\times10^{-5}$ for SINE and LINE) (Figs. 2C and E). These results showed that promoter CGIs located remotely from SINE and LINE are more susceptible to aberrant methylation induction than those located closely to them.

2.3. Promoter CGIs with tissue-nonspecific susceptibility are located more distant from SINE and LINE than promoter CGIs with tissue-specific susceptibility

One hundred and fifty-four promoter CGIs were susceptible both in the prostate and mammary glands (tissue-nonspecific susceptibility). On the other hand, 62 promoter CGIs were susceptible only in the prostate and resistant or intermediate in the mammary glands, and 55 were susceptible only in the mammary glands and resistant or intermediate in the prostate (tissue-specific susceptibility) (Fig. 1B). The promoter CGIs with tissue-nonspecific susceptibility were located significantly more remotely from SINE (P = 0.005) and LINE (P = 0.026) than promoter CGIs with tissue-specific susceptibility in the prostate (Fig. 3A). The same tendency was observed in the mammary glands (Fig. 3B), but the difference was not statistically significant. These results indicated that the promoting effect of the remote location from SINE and LINE on aberrant methylation induction, or protective effect of the close location, is more evident for tissue-nonspecific susceptibility than for tissue-specific susceptibility.

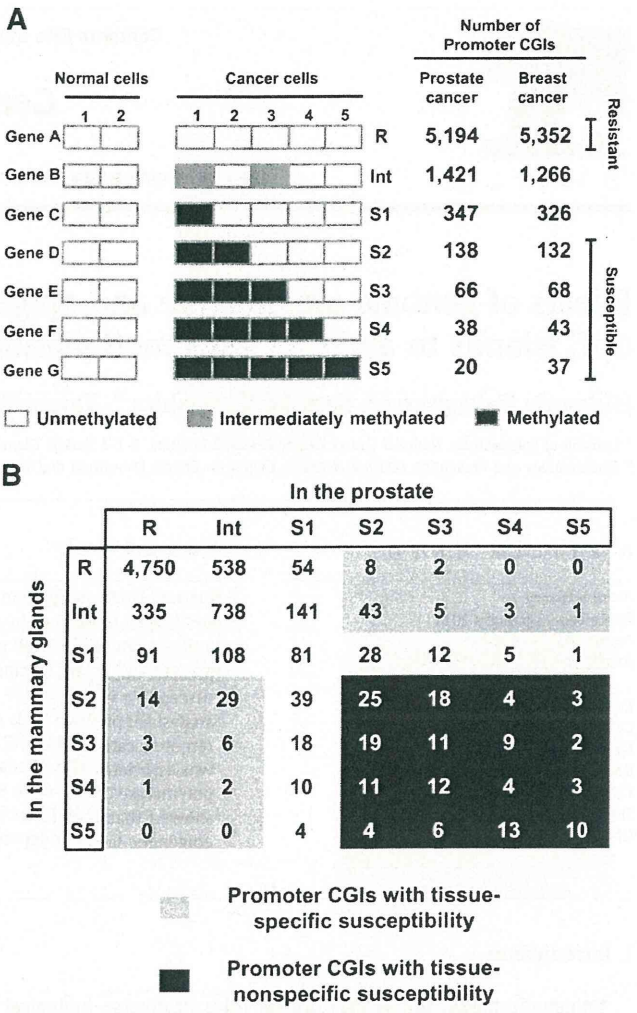

Fig. 1. Classification of promoter CGIs into those susceptible and resistant to aberrant DNA methylation induction, and classification of susceptible promoter CGIs into those with tissue-nonspecific and -specific susceptibility. (A) Classification of promoter CGIs into those susceptible and resistant to aberrant methylation induction. Promoter CGIs unmethylated (white) in both of the two normal cells and methylated (black) in one to five cancer cell lines were classified into Groups S1 to S5. Those unmethylated in both of the two normal cells and also in all cancer cell lines were classified into Group R. Those unmethylated in both of the two normal cells and intermediately methylated (gray) at least in one of the five cancer cell lines were classified into the intermediate group (Int). Promoter CGIs in Groups S2 to S5 and in Group R were considered to be susceptible and resistant, respectively, to aberrant methylation induction. In the prostate, a total of 262 and 5194 promoter CGIs were susceptible and resistant, respectively. In the mammary glands, a total of 280 and 5352 promoter CGIs were susceptible and resistant, respectively. (B) Classification of susceptible promoter CGIs into promoter CGIs with tissue-nonspecific and -specific susceptibility. A total of 154 promoter CGIs were susceptible both in the prostate and mammary glands (black), and 62 and 55 were susceptible only in the prostate and mammary glands, respectively (gray).

2.4. Effects of genome architecture are independent from those of epigenetic factors

Epigenetic factors, such as the presence of Pol II and H3K27me3, are known to be involved in the target gene specificity of aberrant DNA methylation induction [11]. To evaluate whether the effect of genome architecture is independent from those of epigenetic factors, multivariate logistic regression analysis was performed. In the prostate (Table 1), a remote location from SINE [Multivariate-adjusted odds ratio (OR) = 5.98; 95% confidence interval (CI) = 2.33–15.34]

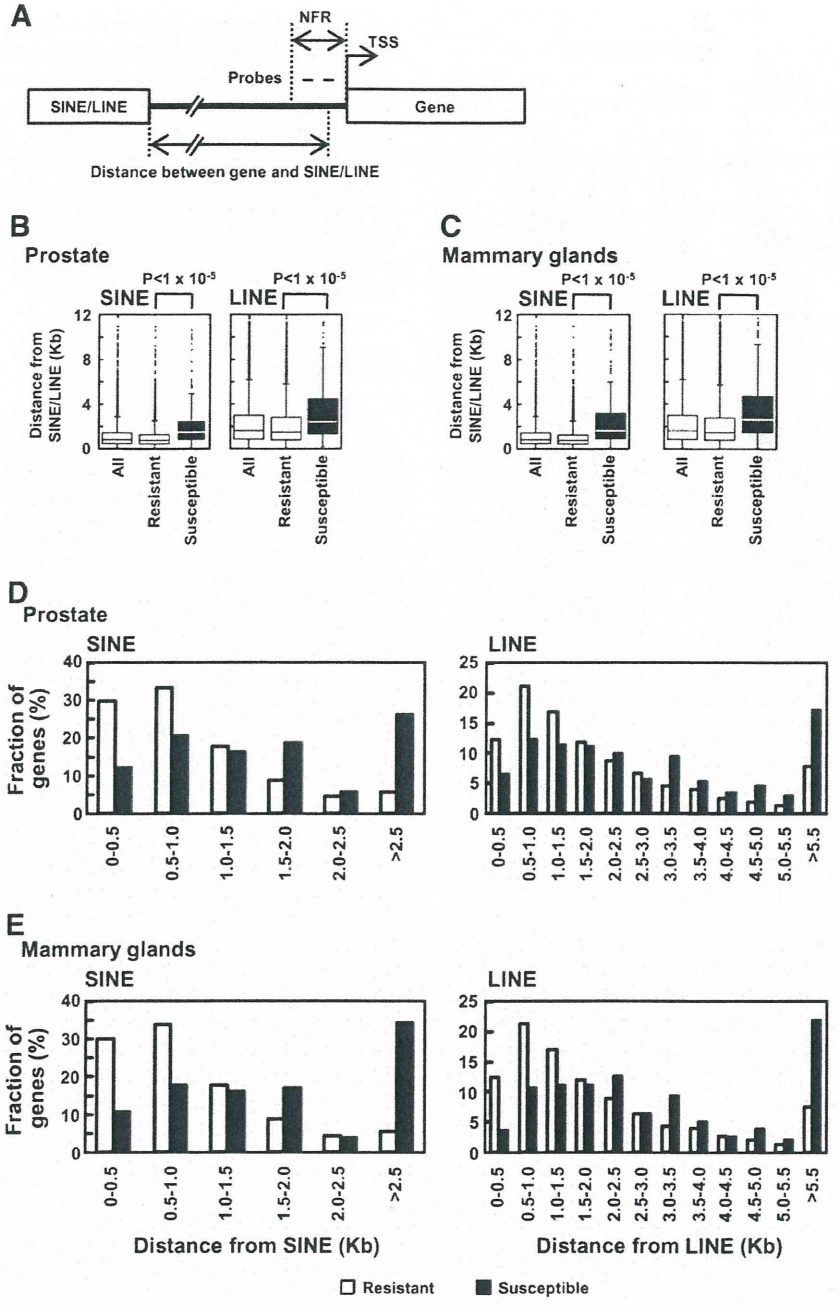

Fig. 2. The effect of remote location from SINE and LINE on aberrant DNA methylation induction during carcinogenesis. (A) The definition of the distance from SINE (or LINE) to the promoter CGI of a gene. The distance from the proximal edge of SINE (or LINE) to the center of the probe (45 to 60 bp in length) nearest to the TSS was defined as the distance from SINE (or LINE) to the promoter CGI of a gene. NFR, nucleosome free region. (B) and (C) the distances from SINE (or LINE) to all, resistant, and susceptible promoter CGIs in the prostate (B) and mammary glands (C). The boxes represent the 75th and 25th percentiles, and the line in the box represents the 50th percentile (the median). Whiskers represent the maximum data within [75th percentile + 1.5 × (75th percentile − 25th percentile)] and the minimum data within [25th percentile − 1.5 × (75th percentile − 25th percentile)]. The data not included between the whiskers are indicated by dots. Susceptible promoter CGIs were located significantly more remotely from SINE and LINE than resistant promoter CGIs in both tissues. (D) and (E) The distribution of resistant and susceptible promoter CGIs from SINE and LINE in the prostate (D) and mammary glands (E). The fractions of resistant (white) and susceptible (black) promoter CGIs in respective distances from SINE and LINE are shown.

and LINE (2.08; 1.03–4.21) retained significant effects on tissue-nonspecific susceptibility (Table 1, the highest quintiles). The presence of Pol II (0.09; 0.02–0.48) and H3K27me3 (3.28; 1.17–9.21) weakly retained independent protective and promoting effects, respectively. Regarding the effects on tissue-specific susceptibility, a remote location from SINE and LINE did not retain the effects while the promoting effect of H3K27me3 was evident (3.34; 1.02–10.94).

Also in the mammary glands (Table 2), a remote location retained independent effects more clearly on tissue-nonspecific susceptibility than on tissue-specific susceptibility.

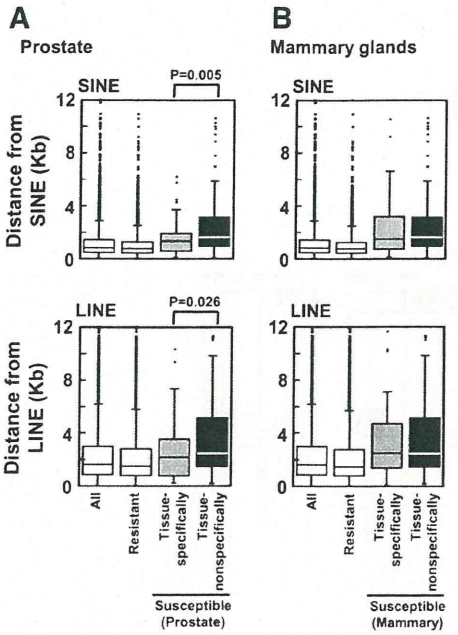

Fig. 3. The effect of remote location from SINE and LINE on tissue-nonspecific and tissue-specific susceptibility. Distance from SINE and LINE to all, resistant, tissue-specifically susceptible, and tissue-nonspecifically susceptible promoter CGIs in the prostate (A) and mammary glands (B). For the box plots, refer to the legend of Fig. 2B. Tissue-nonspecifically susceptible promoter CGIs were located significantly more remotely from SINE and LINE than tissue-specifically susceptible promoter CGIs in the prostate.

2.5. Genes influenced by genome architecture and epigenetic factors have different characteristics

To reveal the characteristics of promoter CGIs whose susceptibility was influenced mainly by genome architecture and those influenced by epigenetic factors, gene ontology analysis of these promoter CGIs was conducted. As promoter CGIs whose susceptibility was influenced mainly by genome architecture, those located remotely from both SINE (>2.5 kb) and LINE (>5.5 kb) and had high Pol II and low H3K27me3 in normal cells were selected. As promoter CGIs whose susceptibility was influenced mainly by epigenetic factors, promoter CGIs located closely to both SINE (<1.0 kb) and LINE (<1.5 kb) and had low Pol II and high H3K27me3 in normal cells were selected.

In the prostate, among genes whose susceptibility was influenced mainly by genome architecture, biological processes involved in early developmental processes such as organ morphogenesis and anterior/posterior pattern formation were enriched. Among genes whose susceptibility was influenced mainly by epigenetic factors, biological processes involved in basic cellular processes in specific cell types such as neurotransmitter transport and amine transport were enriched (Table 3). A similar result was also observed in the mammary glands.

3. Discussion

In this study, we confirmed that a remote location from SINE and LINE is associated with susceptibility of promoter CGIs to become aberrantly methylated during carcinogenesis. Further, we showed that the effect of genome architecture was more evident for tissue-nonspecific susceptibility than for tissue-specific susceptibility, and independent from those of epigenetic factors such as the presence of Pol II and H3K27me3.

The protective effect of the close location to SINE and LINE can be explained by the establishment of active chromatin. Some repetitive sequences are known to be bound by transcription factors, and form active chromatin that eventually protects CGIs from aberrant DNA methylation induction. For example, SINE is known to contain binding sites of YY1 transcription factor [25], which is known to interact with histone acetyltransferases such as CBP (encoded by CREBBP) and p300 (encoded by EP300) [26,27]. Surrounding regions of SINE bound by YY1 are expected to be marked with active histone modifications.

Genes whose susceptibility was influenced mainly by genome architecture had functions involved in early developmental processes. Since genes involved in early developmental processes are considered to be unnecessary in differentiated cells of most tissues, methylation susceptibility of these genes is likely to be determined solely by genome architecture. In contrast, genes whose susceptibility was influenced mainly by epigenetic factors had functions involved in basic cellular processes in specific cell types. Since such genes are utilized in specific tissues, it is expected that such genes have different epigenetic modifications in various normal tissues, and that methylation susceptibility of such genes will be determined mainly by epigenetic factors.

Table 1
The association between the distance from SINE, from LINE, or epigenetic factors and DNA methylation susceptibility in the prostate.

	Lowest quintile	2nd quintile	3rd quintile	4th quintile	Highest quintile
Tissue-nonspecific susceptibility					
The distance from SINE	1	**3.28 (1.18–9.13)**	2.61 (0.91–7.46)	**5.17 (1.96–13.60)**	**5.98 (2.33–15.34)**
The distance from LINE	1	1.12 (0.51–2.47)	1.58 (0.75–3.30)	1.58 (0.76–3.27)	**2.08 (1.03–4.21)**
Transcription	1	0.86 (0.55–1.36)	**0.39 (0.19–0.83)**	0.60 (0.28–1.26)	**0.28 (0.10–0.83)**
H3Ac	1	0.73 (0.41–1.30)	0.53 (0.25–1.12)	0.67 (0.28–1.56)	1.04 (0.37–2.92)
H3K4me3	1	1.19 (0.70–2.03)	0.76 (0.38–1.52)	1.04 (0.49–2.17)	0.80 (0.34–1.84)
Pol II	1	0.58 (0.34–1.02)	**0.23 (0.10–0.57)**	0.42 (0.17–1.05)	**0.09 (0.02–0.48)**
H3K9me3	1	1.74 (0.84–3.60)	1.53 (0.73–3.21)	1.57 (0.75–3.28)	1.15 (0.54–2.47)
H3K27me3	1	1.38 (0.47–4.10)	1.05 (0.35–3.20)	0.60 (0.18–1.99)	**3.28 (1.17–9.21)**
Tissue-specific susceptibility					
The distance from SINE	1	1.25 (0.46–3.40)	1.07 (0.38–2.99)	1.49 (0.57–3.87)	1.87 (0.75–4.68)
The distance from LINE	1	**0.33 (0.12–0.93)**	0.53 (0.22–1.27)	0.74 (0.34–1.65)	0.84 (0.39–1.83)
Transcription	1	0.85 (0.42–1.73)	0.44 (0.17–1.16)	0.51 (0.19–1.39)	0.79 (0.32–1.98)
H3Ac	1	0.50 (0.19–1.30)	0.48 (0.16–1.44)	0.72 (0.24–2.15)	1.26 (0.38–4.20)
H3K4me3	1	1.43 (0.58–3.56)	1.74 (0.67–4.52)	1.29 (0.45–3.66)	1.73 (0.62–4.79)
Pol II	1	0.56 (0.22–1.45)	0.96 (0.37–2.50)	0.32 (0.09–1.15)	0.38 (0.10–1.43)
H3K9me3	1	0.98 (0.43–2.20)	0.49 (0.19–1.26)	**0.37 (0.14–0.99)**	**0.35 (0.13–0.94)**
H3K27me3	1	1.18 (0.35–3.95)	2.35 (0.74–7.44)	**3.45 (1.07–11.15)**	**3.34 (1.02–10.94)**

The association with tissue-nonspecific susceptibility and tissue-specific susceptibility was analyzed separately. Multivariate-adjusted odds ratio (OR) (95% confidence interval; 95% CI) for a CGI in a quintile to become methylated compared with a CGI in a reference quintile (lowest quintile) was calculated by multivariate logistic regression analysis involving all the variables listed. Significant ORs are shown in bold.

Table 2
The association between the distance from SINE, from LINE, or epigenetic factors and DNA methylation susceptibility in the mammary glands.

	Lowest quintile	2nd quintile	3rd quintile	4th quintile	Highest quintile
Tissue-nonspecific susceptibility					
The distance from SINE	1	**3.35 (1.21–9.30)**	2.73 (0.96–7.79)	**5.66 (2.16–14.81)**	**6.31 (2.46–16.17)**
The distance from LINE	1	1.25 (0.57–2.73)	1.68 (0.80–3.50)	1.74 (0.84–3.57)	**2.07 (1.02–4.18)**
Transcription	1	**0.54 (0.32–0.92)**	**0.30 (0.14–0.63)**	**0.31 (0.14–0.68)**	**0.25 (0.10–0.62)**
H3Ac	1	0.76 (0.43–1.35)	0.52 (0.23–1.17)	1.05 (0.43–2.58)	2.25 (0.77–6.57)
H3K4me3	1	1.06 (0.64–1.78)	0.52 (0.24–1.13)	0.77 (0.34–1.74)	0.57 (0.22–1.44)
Pol II	1	0.64 (0.37–1.12)	0.63 (0.31–1.31)	**0.22 (0.08–0.64)**	**0.19 (0.06–0.65)**
H3K9me3	1	1.45 (0.82–2.57)	1.26 (0.69–2.30)	1.21 (0.65–2.25)	0.86 (0.44–1.68)
H3K27me3	1	0.45 (0.18–1.13)	0.62 (0.27–1.42)	0.56 (0.24–1.33)	2.00 (0.96–4.17)
Tissue-specific susceptibility					
The distance from SINE	1	2.00 (0.49–8.08)	2.38 (0.61–9.33)	2.42 (0.64–9.17)	**3.78 (1.07–13.31)**
The distance from LINE	1	1.14 (0.30–4.29)	1.87 (0.56–6.17)	1.89 (0.58–6.20)	2.93 (0.95–8.99)
Transcription	1	**0.32 (0.13–0.79)**	**0.14 (0.04–0.51)**	**0.19 (0.06–0.60)**	**0.12 (0.03–0.45)**
H3Ac	1	1.01 (0.36–2.79)	1.35 (0.40–4.53)	1.44 (0.35–5.88)	1.91 (0.35–10.33)
H3K4me3	1	0.69 (0.28–1.68)	0.49 (0.16–1.51)	**0.23 (0.06–0.93)**	0.23 (0.05–1.08)
Pol II	1	1.08 (0.42–2.80)	0.80 (0.21–3.03)	2.25 (0.62–8.10)	1.86 (0.37–9.44)
H3K9me3	1	0.47 (0.17–1.28)	0.92 (0.39–2.19)	0.78 (0.31–1.96)	0.47 (0.16–1.38)
H3K27me3	1	1.57 (0.47–5.26)	1.35 (0.39–4.71)	1.22 (0.33–4.54)	2.02 (0.61–6.74)

Using the data in the mammary glands, multivariate analyses were performed as in Table 1. Significant ORs are shown in bold.

To identify promoter CGIs susceptible across tissues and specifically in a tissue, two tissues, the prostate and mammary glands, were analyzed. Despite the limited number of analyzed tissues, the stronger effect of genome architecture on tissue-nonspecifically susceptible promoter CGIs than on tissue-specifically susceptible promoter CGIs could be observed. Nevertheless, the number of tissues analyzed was still small to isolate a pure population of tissue-nonspecifically susceptible promoter CGIs. It is expected that the stronger effect of genome architecture will become more evident when a larger number of tissues are analyzed.

For identification of DNA methylation-susceptible and -resistant promoter CGIs, we analyzed methylation statuses of cancer cell lines. It is known that cancer cell lines generally have a larger number of methylated genes than primary tumors. However, it was observed that, when a large number of primary tumors were analyzed, most methylation found in cancer cell lines was present also in a minor fraction of the primary tumors [28–30]. Therefore, it is considered that methylation susceptibility observed in cancer cell lines reflects that in primary tumors as a whole.

In conclusion, DNA methylation susceptibility of promoter CGIs is determined by genome architecture and epigenetic factors, independently.

4. Materials and methods

4.1. Cell lines

A normal prostatic epithelial cell line (RWPE1), prostate cancer cell lines (PC3, LNCaP, 22Rv1, Du145, and MDA-PCa-2b), and breast cancer cell lines (BT474, MCF7, MDA-MB-231, MDA-MB-468, and ZR-75-1) were obtained from the American Type Culture Collection (Rockville, MD). Normal human prostate epithelial cells (PrEC) were obtained from Lonza (Walkersville, MD). Normal human mammary epithelial cells (HMECs) were obtained from Cambrex (East Rutherford, NJ). PrEC was maintained in PrEGM BulletKit (Lonza), BT474 and MDA-MB-231 were maintained in RPMI1640, and other cells were maintained as described previously [11].

4.2. Analysis of DNA methylation

DNA methylation data of RWPE1, PC3, LNCaP, 22Rv1, Du145, HMEC (lot. OF1330), MCF7, MDA-MB-468, and ZR-75-1 were obtained in our previous study [11]. Methylation statuses of PrEC, MDA-PCa-2b, HMEC (lot. 0000092969), BT474, and MDA-MB-231 were newly analyzed in this study as described previously [11,31]. DNA immunoprecipitated by antibody against 5-methylcytidine (Diagnode, Liége, Belgium) was analyzed by human CGI microarray (Agilent Technologies, Santa Clara, CA) that contained 27,800 CGIs, 9838 of which were located within 200 bp upstream from TSSs, and thus in promoter regions. The methylation level of each probe was evaluated using Me values ranging from 0 (completely unmethylated) to 1 (fully methylated) [31]. The methylation status of each gene was defined as unmethylated, intermediately methylated, and methylated when the average of the Me value of probes within a NFR (defined as a region between a TSS and its 200 bp upstream) was 0–0.4, 0.4–0.6, and 0.6–1.0, respectively [11]. Methylation data of PrEC, MDA-PCa-2b,

Table 3
Functional annotation analysis of genes whose susceptibility was influenced by genome architecture or epigenetic factors.

Category	Prostate		Mammary glands	
	Term	P value	Term	P value
Genes whose susceptibility was influenced by genome architecture	Skeletal system morphogenesis	1.93E−06	Anterior/posterior pattern formation	3.79E−06
	Organ morphogenesis	2.52E−06	Regionalization	1.06E−05
	Anterior/posterior pattern formation	3.79E−06	Pattern specification process	2.64E−05
	Regionalization	1.06E−05	Embryonic morphogenesis	4.01E−05
	Pattern specification process	2.64E−05	Organ development	2.29E−04
Genes whose susceptibility was influenced by epigenetic factors	Neurotransmitter transport	2.91E−02	Neurotransmitter transport	3.48E−02
	Response to external stimulus	3.67E−02	Amine transport	4.91E−02
	Amine transport	4.11E−02		
	Transport	4.79E−02		
	Regulation of body fluid levels	4.90E−02		

Enrichment of specific biological processes in Gene Ontology criteria among genes whose susceptibility was influenced by genome architecture (n = 6 in the prostate; n = 5 in the mammary glands) or epigenetic factors (n = 9 in the prostate; n = 9 in the mammary glands) was analyzed by DAVID bioinformatics resources. The top five significantly enriched biological processes in each gene category are listed. The significance (P value) of enrichment is shown.

HMEC (lot. 0000092969), BT474, and MDA-MB-231 were submitted to the GEO database under accession no. GSE28284.

4.3. Determination of the distance from SINE (or LINE) to the promoter CGI of a gene

The position information of SINE and LINE was obtained from UCSC hg18 (NCBI Build 36.1, March 2006). The distance from the proximal edge of SINE (or LINE) to the center of the probe (45 to 60 bp in length) nearest the TSS located within a NFR was defined as the distance from SINE (or LINE) to the promoter CGI of a gene (Fig. 2A).

4.4. Analyses of transcription level, histone modifications, and Pol II binding

Transcription levels, histone modifications, and Pol II binding in normal cells, RWPE1 and HMEC (lot. OF1330), were obtained from our previous study [11]. Transcription levels were analyzed using the GeneChip Human Genome U133 Plus 2.0 microarray (Affymetrix, Santa Clara, CA). Histone modifications and Pol II binding were analyzed by chromatin immunoprecipitation combined with a human CGI microarray. Histone modifications and the Pol II binding level of each gene were evaluated by the average of Cy5/Cy3 (bound/input) signal ratio of probes within NFR. Genes were classified into those with high and low levels of H3K27me3 or Pol II binding when they had signal ratios higher and lower, respectively, than the average signal ratio of total probes.

4.5. Functional annotation analysis

Functional annotation analysis was performed by DAVID bioinformatics resources [32,33]. The enrichment of genes in a biological process (a Gene Ontology criterion) was analyzed by comparing a fraction of genes with an ontology among genes whose susceptibility was influenced by genome architecture (or by epigenetic factors) with that among all the genes.

4.6. Multivariate analysis and statistical tests

Multivariate logistic regression analysis was conducted using DNA methylation susceptibility as an outcome variable. The predictor variables [transcription, acetylation of histone H3 (H3Ac), trimethylation of histone H3 lysine4 (H3K4me3), Pol II binding, trimethylation of histone H3 lysine9 (H3K9me3), H3K27me3, the distance from SINE, and that from LINE] were categorized into quintiles according to their values [transcription levels, histone modification levels and Pol II binding levels in RWPE1 or HMEC (lot. OF1330), and the distance from SINE (or LINE) to the promoter CGI] to create dummy variables. OR and 95% CI of methylation susceptibility of genes in each quintile, using the lowest quintile as a reference, were calculated, including all predictor variables simultaneously in the model using SAS software, ver. 9.1 (SAS Institute Inc, SAS/STAT 9.1 user's guide, SAS Institute Inc, Cary, NC). These ORs show a probability for a gene in a quintile to become methylated, relative to the lowest quintile, after controlling the effect of all the other predictor variables included in the model. 95% CIs show the range into which the true OR falls with a chance of 95% or greater. The distances from SINE and LINE in different groups of genes were compared by the Mann–Whitney U-test.

Acknowledgments

This work was supported by Grants-in-Aid for the Third-Term Comprehensive Cancer Control Strategy from the Ministry of Health, Labour and Welfare, Japan; for Young Scientists (B) from Japan Society for the Promotion of Science (JSPS); and a grant from the Foundation for Promotion of Cancer Research. We thank Dr. Toshiki Taya (Agilent Technology) for his support in calculating the distance from SINE and LINE to each probe.

References

[1] A. Bird, DNA methylation patterns and epigenetic memory, Genes Dev. 16 (2002) 6–21.
[2] T. Ito, Role of histone modification in chromatin dynamics, J. Biochem. 141 (2007) 609–614.
[3] T. Kouzarides, Chromatin modifications and their function, Cell 128 (2007) 693–705.
[4] P.W. Laird, R. Jaenisch, The role of DNA methylation in cancer genetic and epigenetics, Annu. Rev. Genet. 30 (1996) 441–464.
[5] P.A. Jones, S.B. Baylin, The epigenomics of cancer, Cell 128 (2007) 683–692.
[6] H. Soejima, W. Zhao, T. Mukai, Epigenetic silencing of the MGMT gene in cancer, Biochem. Cell Biol. 83 (2005) 429–437.
[7] T. Ushijima, Detection and interpretation of altered methylation patterns in cancer cells, Nat. Rev. Cancer 5 (2005) 223–231.
[8] J.C. Lin, S. Jeong, G. Liang, D. Takai, M. Fatemi, Y.C. Tsai, G. Egger, E.N. Gal-Yam, P.A. Jones, Role of nucleosomal occupancy in the epigenetic silencing of the MLH1 CpG island, Cancer Cell 12 (2007) 432–444.
[9] T. Nakajima, S. Yamashita, T. Maekita, T. Niwa, K. Nakazawa, T. Ushijima, The presence of a methylation fingerprint of *Helicobacter pylori* infection in human gastric mucosae, Int. J. Cancer 124 (2009) 905–910.
[10] D. Oka, S. Yamashita, T. Tomioka, Y. Nakanishi, H. Kato, M. Kaminishi, T. Ushijima, The presence of aberrant DNA methylation in noncancerous esophageal mucosae in association with smoking history: a target for risk diagnosis and prevention of esophageal cancers, Cancer 115 (2009) 3412–3426.
[11] H. Takeshima, S. Yamashita, T. Shimazu, T. Niwa, T. Ushijima, The presence of RNA polymerase II, active or stalled, predicts epigenetic fate of promoter CpG islands, Genome Res. 19 (2009) 1974–1982.
[12] C. De Smet, A. Loriot, T. Boon, Promoter-dependent mechanism leading to selective hypomethylation within the 5′ region of gene MAGE-A1 in tumor cells, Mol. Cell. Biol. 24 (2004) 4781–4790.
[13] J. Furuta, Y. Nobeyama, Y. Umebayashi, F. Otsuka, K. Kikuchi, T. Ushijima, Silencing of Peroxiredoxin 2 and aberrant methylation of 33 CpG islands in putative promoter regions in human malignant melanomas, Cancer Res. 66 (2006) 6080–6086.
[14] A. Hagihara, K. Miyamoto, J. Furuta, N. Hiraoka, K. Wakazono, S. Seki, S. Fukushima, M.S. Tsao, T. Sugimura, T. Ushijima, Identification of 27 5′ CpG islands aberrantly methylated and 13 genes silenced in human pancreatic cancers, Oncogene 23 (2004) 8705–8710.
[15] J.Z. Song, C. Stirzaker, J. Harrison, J.R. Melki, S.J. Clark, Hypermethylation trigger of the glutathione-S-transferase gene (GSTP1) in prostate cancer cells, Oncogene 21 (2002) 1048–1061.
[16] Y. Kondo, L. Shen, A.S. Cheng, S. Ahmed, Y. Boumber, C. Charo, T. Yamochi, T. Urano, K. Furukawa, B. Kwabi-Addo, D.L. Gold, Y. Sekido, T.H. Huang, J.P. Issa, Gene silencing in cancer by histone H3 lysine 27 trimethylation independent of promoter DNA methylation, Nat. Genet. 40 (2008) 741–750.
[17] J.E. Ohm, K.M. McGarvey, X. Yu, L. Cheng, K.E. Schuebel, L. Cope, H.P. Mohammad, W. Chen, V.C. Daniel, W. Yu, D.M. Berman, T. Jenuwein, K. Pruitt, S.J. Sharkis, D.N. Watkins, J.G. Herman, S.B. Baylin, A stem cell-like chromatin pattern may predispose tumor suppressor genes to DNA hypermethylation and heritable silencing, Nat. Genet. 39 (2007) 237–242.
[18] Y. Schlesinger, R. Straussman, I. Keshet, S. Farkash, M. Hecht, J. Zimmerman, E. Eden, Z. Yakhini, E. Ben-Shushan, B.E. Reubinoff, Y. Bergman, I. Simon, H. Cedar, Polycomb-mediated methylation on Lys27 of histone H3 pre-marks genes for de novo methylation in cancer, Nat. Genet. 39 (2007) 232–236.
[19] M.A. Hahn, T. Hahn, D.H. Lee, R.S. Esworthy, B.W. Kim, A.D. Riggs, F.F. Chu, G.P. Pfeifer, Methylation of polycomb target genes in intestinal cancer is mediated by inflammation, Cancer Res. 68 (2008) 10280–10289.
[20] M.T. McCabe, E.K. Lee, P.M. Vertino, A multifactorial signature of DNA sequence and polycomb binding predicts aberrant CpG island methylation, Cancer Res. 69 (2009) 282–291.
[21] H. Takeshima, T. Ushijima, Methylation destiny: Moira takes account of histones and RNA polymerase II, Epigenetics 5 (2010) 89–95.
[22] C. Gebhard, C. Benner, M. Ehrich, L. Schwarzfischer, E. Schilling, M. Klug, W. Dietmaier, C. Thiede, E. Holler, R. Andreesen, M. Rehli, General transcription factor binding at CpG islands in normal cells correlates with resistance to de novo DNA methylation in cancer cells, Cancer Res. 70 (2010) 1398–1407.
[23] F.A. Feltus, E.K. Lee, J.F. Costello, C. Plass, P.M. Vertino, DNA motifs associated with aberrant CpG island methylation, Genomics 87 (2006) 572–579.
[24] M.R. Estecio, J. Gallegos, C. Vallot, R.J. Castoro, W. Chung, S. Maegawa, Y. Oki, Y. Kondo, J. Jelinek, L. Shen, H. Hartung, P.D. Aplan, B.A. Czerniak, S. Liang, J.P. Issa, Genome architecture marked by retrotransposons modulates predisposition to DNA methylation in cancer. Genome Res. 20 (2010) 1369–1382.
[25] N.V. Tomilin, Regulation of mammalian gene expression by retroelements and non-coding tandem repeats, Bioessays 30 (2008) 338–348.
[26] S. Gordon, G. Akopyan, H. Garban, B. Bonavida, Transcription factor YY1: structure, function, and therapeutic implications in cancer biology, Oncogene 25 (2006) 1125–1142.
[27] M.J. Thomas, E. Seto, Unlocking the mechanisms of transcription factor YY1: are chromatin modifying enzymes the key? Gene 236 (1999) 197–208.
[28] D. Lodygin, A. Epanchintsev, A. Menssen, J. Diebold, H. Hermeking, Functional epigenomics identifies genes frequently silenced in prostate cancer, Cancer Res. 65 (2005) 4218–4227.

[29] N. Sato, N. Fukushima, A. Maitra, H. Matsubayashi, C.J. Yeo, J.L. Cameron, R.H. Hruban, M. Goggins, Discovery of novel targets for aberrant methylation in pancreatic carcinoma using high-throughput microarrays, Cancer Res. 63 (2003) 3735–3742.
[30] S. Yamashita, Y. Tsujino, K. Moriguchi, M. Tatematsu, T. Ushijima, Chemical genomic screening for methylation-silenced genes in gastric cancer cell lines using 5-aza-2′-deoxycytidine treatment and oligonucleotide microarray, Cancer Sci. 97 (2006) 64–71.
[31] S. Yamashita, K. Hosoya, K. Gyobu, H. Takeshima, T. Ushijima, Development of a novel output value for quantitative assessment in methylated DNA immunoprecipitation-CpG island microarray analysis, DNA Res. 16 (2009) 275–286.
[32] G. Dennis Jr., B.T. Sherman, D.A. Hosack, J. Yang, W. Gao, H.C. Lane, R.A. Lempicki, DAVID: database for annotation, visualization, and integrated discovery, Genome Biol. 4 (2003) P3.
[33] W. Huang da, B.T. Sherman, R.A. Lempicki, Systematic and integrative analysis of large gene lists using DAVID bioinformatics resources, Nat. Protoc. 4 (2009) 44–57.

Tokai J Exp Clin Med., Vol. 36, No. 3, pp. 84-90, 2011

Does Aberrant DNA Methylation Occur in Human Uterine Leiomyomas? An Attempt of Genome-Wide Screening by MS-RDA

Li-Yi CAI[*1][*2], Shun-ichiro IZUMI[*1][*3], Masanobu ABE[*2], Masayoshi IMURA[*2][*4], Toshiharu YASUGI[*4], Kuniko WAKAZONO[*2], Yuko OHNUKI[*3], Akane KONDO[*1][*3] and Toshikazu USHIJIMA[*2]

[*1]*Department of Obstetrics and Gynecology, Tokai University School of Medicine*
[*2]*Carcinogenesis Division, National Cancer Center Research Institute*
[*3]*Department of clinical Genetics, Tokai University Hospital*
[*4]*Department of Obstetrics and Gynecology, The University of Tokyo Graduate School of Medicine*

(Received November 10, 2010; Accepted July 25, 2011)

Objective : Uterine leiomyoma are very common benign tumors in women of reproductive age. However, the molecular mechanisms of cause and development of these tumors are poorly understood. This study attempts to examine whether or not aberrant DNA methylation occurred in these tumors.
Methods : We carried out a genome-wide screen for aberrant DNA methylation, adopting methylation-sensitive-representational difference analysis (MS-RDA) using normal adjacent myometria as tester and myoma tissue driver.
Conclusion : A total of 192 clones identified by MS-RDA were sequenced, 27 DNA fragments derived from CpG islands (CGIs) were isolated, and seven of them were from CGI in the 5' regions of known genes, which include CHARC1, FAM44B, FLJ33655, HSUP, MLLT3, SLC16A1, and ZNF96. Then, methylation statuses of those CGIs were analyzed by methylation-specific polymerase chain reaction using 5 primary samples of human uterine leiomyoma. Aberrant DNA methylation did not observed in 7 genes in 5 human uterine leiomyoma eventually. This study is insufficient to identify aberrant DNA methylation occurring in the human uterine leiomyoma, a large population of primary samples and more attempts, such as the use of cell lines or primary monolayer cultures established from tissue samples, are warranted to clarify this issue.

Key words: MS-RDA, uterine leiomyoma, CpG island, DNA methylation

INTRODUCTION

Uterine leiomyomas are the most common benign gynecological tumor and occur in 25% of women of reproductive age [1]. Various clinical problems such as pelvic pain, abnormal uterine bleeding, urinary frequency, infertility, and recurrent pregnancy loss are attributed to this disease [2, 3]. Though remarkably literature about their epidemiology, cytogenetics, molecular genetics and hormonal aspects are published [4-7], the molecular mechanisms of cause of these tumors remain unclear. Previous studies suggest that uterine leiomyomas are monoclonal tumors that origin from smooth muscle cells [8]. Cytogenetic analyses showed that some chromosome are changed, such as trisomy 12, translocation between chromosome 12 and 14, deletions of chromosomes 3 and 7, rearrangement of short arm of chromosome 6 and of the long arm of chromosome 10 [4, 9]. In addition, increasing evidence has demonstrated that sex steroid hormones and growth factors play central roles in leiomyoma development and growth [7, 10-12]. Since the steroid hormone levels in women with leiomyoma are similar to those in normal women, sex steroids are not considered to be the sole modulators of tumorigenesis [13]. Therefore, the underling molecular mechanisms for tumorigenesis remain to be elucidated.

Alterations of DNA-methylation patterns, as an epigenetic modulation, both the regional hypermethylation and the global hypomethylation in genomic DNA, are deeply involved in many human tumor types [14]. DNA methylation defined as methylation of the C5 position of cytosine/guanine pairs (CpG) in DNA, and has been observed in CG-rich region, called CpG islands (CGIs), frequently located in a promoter. These CGIs are normally kept free of methylation in promoter regions for proteins binding and initiating gene transcription. However, methylated CGIs lead to stable heritable transcriptional silencing of tumor-suppressor genes and have been considered as common features in human carcinomas [15]. Moreover, aberrant DNA methylation was also shown to be present in noncancerous mucosae of ulcerative colitis and H. pylori-infected gastric mucosae in previous studies [16, 17], a role of chronic inflammation in methylation induction was proposed.

On the other hand, global hypomethylation frequently targeted repetitive sequences [18] have been demonstrated to contribute to tumorigenesis and progression through effects on chromosomal stability [19]. Li *et al.* demonstrated that global DNA hypomethylation and differential expressions of different DNA

Shun-ichiro IZUMI, Gynecology, Tokai University School of Medicine, 143 Shimokasuya, Isehara, Kanagawa 259-1193, Japan
Tel: +81-463-93-1121 Fax: +81-463-91-4343 E-mail: s-izumi@is.icc.u-tokai.ac.jp

methyltransferases (DNMT1, 3A and 3B) in uterine leiomyoma tissue as compared with the adjacent myometria, suggesting a potential mechanism of epigenetic modulation in the development of this tumor [20]. Moreover, aberrant promoter methylation of cancer-related genes has been detected in leiomyosarcomas, such as ERa (80%), DAP kinase (54%), RASSF1A (39%), p16INK4a (22%-25%), and MLH1 (6%) [21-23]. Therefore, it is of interesting to investigate whether aberrant DNA methylation is involved in the development of the benign tumor of human leiomyoma.

For this purpose, we adopted a genome-wide screening for differences in DNA methylation, methylation-sensitive-representational difference analysis (MS-RDA) [24-26]. MS-RDA is a power technique to isolate differentially methylated DNA fragments between two genomes. In MS-RDA, genomic DNA is first digested with a methylation-sensitive restriction enzyme that has a four-base or six-base recognition sequence, such as HpaII, SacII, or NarI. And genomic DNA can be only cut at unmethylated recognition sites. Then an adaptor is ligated to the restricted site. The ligation products are then PCR amplified using the adaptor as primer. This procedure produces a DNA fragments library derived from unmethylated CpG-rich regions of the genome, while miss to produce a library derived from methylated CpG-rich of the genome because that methylation-sensitive restriction enzyme can not cut methylated recognition sites. Therefore, the two different DNA fragment libraries can be isolated by RDA. Adopting MS-RDA technology, it has been successfully to identify various aberrant methylation and silenced genes in human lung cancers [27], stomach cancers [28], pancreatic cancers [29], breast cancers [30, 31], neuroblastomas [32] and ovarian cancers [33].

MATERIALS AND METHODS

Tissue samples and DNA extraction

Leiomyomas were obtained from five patients undergoing surgical treatment for this disease at Tokai University Hospital. Informed consent was obtained from all patients. As normal control, adjacent uterine myometria of 0.5-1.0 cm was collected from the same patient. Tissue samples were stored at -80℃ until used. DNA was extracted by a standard phenol/chloroform and ethanol precipitation procedure.

MS-RDA and database search

For MS-RDA [24, 31], genomic DNA of myoma tissue and adjacent myometria from the identical patient (case 1) was prepared and digested with HpaII, which is a methylation sensitive restriction enzyme that prevented by the presence of a 5-methyl group at the internal C residue of its recognition sequence CCGG. The pooled DNA of myoma tissue was used as driver, and the pooled DNA of adjacent myometria was used as tester in this study. In briefly, R adaptor (RHpa24: 5'-AGCACTCTCCAGCCTCTCA-CCGCA-3'; RHpaII: 5'-CGGTCGGTGAG-3') was ligated to 1 μg of genomic DNA digested with HpaII (New England Biolabs, Beverly, MA, USA). Then the ligation product was amplified by 25 cycles of PCR with RHpa24 oligonucleotide in the presence of 1 M betaine (Sigma, St. Louis, MO, USA). PCR products (amplicon) of both tester and driver were digested with HpaII. J adaptor (JHpa24: 5'-ACCGACGTCGACTATCCATGA-AAC-3'; JHpa11: 5'-CGGTTTCATGG-3') was ligated only to the tester amplicon, and 200 ng of it was mixed with 40 μg of the driver amplicon. Then the mixture underwent heat denaturation and reannealing (competitive hybridization), and dsDNA with the J adaptor on both ends was selectively amplified (selective amplification) with JHpa24 oligonucleotide. The adaptor of the first competitive hybridization and selective amplification was switched to a new N adaptor (NHpa24: 5'-AGGCAACTGTGCTA-TCCGAGGGAC-3'; Nhpa11: 5'-CGGTCCCTCG-G-3'). Ligation product (40 ng) was mixed with 40 μg of driver amplicon, and the second cycle competitive hybridization and selective amplification were carried out. The final product was cloned into the pGEM-T Easy Vector (Promega, Madison, WI, USA), and total 192 clones were sequenced. Their genomic origins were examined by BLASTN software; chromosomal position and relative locations to CGIs were discovered at the GeneBank web site (http://www.ncbi.nlm.nih.gov).

Bisulfite modification and methylation-specific PCR

For sodium bisulfite modification, genomic DNA was restricted with BamHI (New England Biolabs Japan) and purified by phenol extraction. A total of 500 ng restricted DNA was denatured in 0.3 N NaOH at 37℃ for 15 min, then 15 cycles of denaturation was done at 95℃ for 30 sec and incubation at 50℃ for 15 min in 3.1 M NaHSO3 (pH = 5.0) and 0.5 mM hydroquinone. The product was desalted with the Wizard DNA Clean-Up System (Promega Corp., Madison, WI, USA), and desulfonated in 0.6 N NaOH at room temperature for 5 min, then ethanol precipitated and dissolved in 20 μl of TE buffer.

For methylation-specific PCR (MSP) [34], sodium-bisulfite-modified DNA was amplified with primer set specific to the methylated or unmethylated sequences. DNA from human ovarian surface epithelial (HOSE) was methylated in vitro using SssI-methylase (New England Biolabs), and used as a control for methylated DNA. MSP was done in a total volume of 20 μl, containing 1 μl modified template DNA, 1 μM of each primer, 0.2 mM deoxynucleotide triphosphates (Applied Biosystems), 2 μl 10 × PCR buffer with 15 mM Mg2+ (Applied Biosystems), and 0.5 unit AmpliTaq Gold (Applied Biosystems). MSP reactions were subjected to initial incubation at 95℃ for 10 min, followed by cycles of 95℃ for 30 seconds, and annealing at the appropriate temperature for 30 seconds and 72℃ for 30 seconds. To avoid confounding effects of low levels of unmodified DNA, the number of cycles of PCR used did not exceed 35 cycles. The CGIs analyzed are listed in (Table 1). Primer sequences and MSP conditions are detailed in Table 2. MSP products were separated on 2% agarose gels and visualized after ethidium bromide staining.

RESULTS

Isolation of putative aberrantly methylated CGIs by a genome-wide screening

Use of cell lines is commonly recommended for MS-

Table 1 Seven CpG Islands Methylation Analysis in Human Uterine Leiomyoma

Genes			Chromosomal location	Accession number	Map start position	CpG island		
Symbol	Description	Accession number				Length (bp)	%GC	ObsCpG/ ExpCpG*
CHARC1	chromatin accessibility complex 1	NM_017444	8q24.3	AC107375	56761†	2001	67.3	0.94
FAM44B	family with sequence similarity 44, member B	NM_138369	5q35.2	AC010339	95001†	1500	55.1	0.83
FLJ33655	hypothetical protein FLJ33655	NM_173641	1p34.3	AC104336	84609†	900	63.7	0.67
HSUP1	similar to RPE-spondin	XM_49776	20q13.13	AL049766	53976	2001	62.3	0.74
MLLT3	myeloid/lymphoid or mixed lineage-leukemia translocation to 3 homolog	NM_004529	9p22	AL354879	13221†	2001	61.4	0.81
SLC16A1	solute carrier family 16	NM_003051	1p12	AL158844	46763†	2000	62.3	0.80
ZNF96	zinc finger protein 96	NM_014724	6p22.2-p21.3	AC005678	61690†	1000	56.8	0.69

*ObsCpG/ExpCpG: observed CpG/expected CpG ratio; †: Reverse strand

Table 2 Primer Sequences and PCR Conditions for MSP

Genes	Methylation	Forward	Reverse	Annealing temperature (℃)	PCR production length (bp)
CHARC1	M	5'-TTTTCGGTTGTCGGTTTCGC-3'	5'-CCCGATCTACGCATACGCCG-3'	59	75
	U	5'-GATTTTTGGGAGTGGTGT-3'	5'-AAACTCCATAAAAACCTCACA-3'	59	137
FAM44B	M	5'-TAATGTAAAGGTTAACGTTGAC-3'	5'-ATAAAAACGACGACGACG-3'	54	120
	U	5'-ATGTAAAGGTTAATGTTGAT-3'	5'-TAATAAAAAACAACAACAACA-3'	54	120
FLJ33655	M	5'-GGTTGGTATTTCGCGGC-3'	5'-GAACTATCAATCCGACGACG-3'	59	149
	U	5'-ATTGGTTGGTATTTTGTGGT-3'	5'-ACCAAACTATCAATCCAACA-3'	57	155
HSUP1	M	5'-TATCGTTTATTTAGCGTTTC-3'	5'-AAATACTAAAAAAAACGACG-3'	54	132
	U	5'-TATTGTTTATTTAGTGTTTT-3'	5'-AAATACTAAAAAAAACAACA-3'	50	132
MLLT3	M	5'-GAGTTTTTTTTGGTTCGTTC-3'	5'-TAATTACGAAACATACGCCG-3'	56	122
	U	5'-AGTTTTTTTTGGTTTGTTT-3'	5'-TAATTACAAAACATACACCA-3'	53	121
SLC16A1	M	5'-CGTCGTTTAGTAGGGGCGTAGC-3'	5'-GTCTCTCCCGACCGCCG-3'	62	176
	U	5'-TGTTTAGTAGGGGTGTAGTGTGT-3'	5'-CATCTCTCCCAACCACCA-3'	58	174
ZNF96	M	5'-TTTTTTTTTTACGTAGACGC-3'	5'-ACCGAAAACGACCACG-3'	53	127
	U	5'-TTTTTTTTTATGTAGATGTGT-3'	5'-ACAAAAACCAAAAACA-3'	48	131

RDA. Due to few cell lines can be available for human leiomyomas, the primary samples were utilized. MS-RDA was performed with HpaII using a tissue sample from an identical patient. HapII is a methylation sensitive restriction endonuclease and prevented by the presence of a 5-methyl group at the internal C residue of its recognition sequence CCGG. In this study, adjacent myometria was used as the tester and myoma tissue was used as the driver to isolate DNA fragments specifically methylated in myoma tissue. Because methylation of promoter CGI leads to transcriptional silencing of their downstream genes [35, 36], we focus on the CGIs located at 5' region of genes. A total of 192 clones were obtained and sequenced, 62 of them were non-redundant. After BLAST search, 27 clones were found be derived from CGIs, and seven were flanked by CGIs in 5' region of genes (Table 1). Those cloned DNA fragments by MS-RDA, may be putative aberrantly methylated in leiomyoma tissue and their methylation statuses were examined in all five primary patients by MSP.

Methylation analysis of CpG islands in promoter region by MSP

It is considered that, hypermethylation rising in the core region of the 5' CGIs of genes closely correlated with transcriptional inactivation. Therefore, methylation statuses of the core regions in seven isolated genes, CHARC1 (8q24), FAM44B (5q35), FLJ33655 (1p34), HSUP (20q13), MLLT3 (9p12), SLC16A1 (1p12), and ZNF96 (6p22-21) (Table 1 and Fig. 1), were analyzed by MSP in five primary samples and immortalized human ovarian surface cell line (HOSE6-3) as a control. MSP was performed with a primer set specific to methylated or unmethylated sequence (M or U set, Table 2). The MSP results are shown in Fig. 2. The results did not reveal any aberrant DNA methylation of seven genes in 5 patients investigated.

DISCUSSION

In this study, we performed a genome-wide screen to identify aberrant DNA methylation in uterine leiomyoma by MS-RDA technology. A total of 192 clones were sequenced, and 7 genes with 5' CGIs, CHARC1, FAM44B, FLJ33655, HSUP, MLLT3, SLC16A1, and ZNF96 were isolated as putative aberrantly methyla-